



**HAL**  
open science

## Cable tray fire tests with halogenated electric cables in a confined and mechanically ventilated facility

Pascal Zavaleta, Sylvain Suard, Laurent Audouin

### ► To cite this version:

Pascal Zavaleta, Sylvain Suard, Laurent Audouin. Cable tray fire tests with halogenated electric cables in a confined and mechanically ventilated facility. *Fire and Materials*, 2019, 43 (5), pp.543-560. 10.1002/fam.2717 . irsn-04066478

**HAL Id: irsn-04066478**

**<https://irsn.hal.science/irsn-04066478>**

Submitted on 12 Apr 2023

**HAL** is a multi-disciplinary open access archive for the deposit and dissemination of scientific research documents, whether they are published or not. The documents may come from teaching and research institutions in France or abroad, or from public or private research centers.

L'archive ouverte pluridisciplinaire **HAL**, est destinée au dépôt et à la diffusion de documents scientifiques de niveau recherche, publiés ou non, émanant des établissements d'enseignement et de recherche français ou étrangers, des laboratoires publics ou privés.

# CABLE TRAY FIRE TESTS WITH HALOGENATED ELECTRIC CABLES IN A CONFINED AND MECHANICALLY-VENTILATED FACILITY

Pascal Zavaleta, Sylvain Suard, Laurent Audouin

Institut de Radioprotection et de Sûreté Nucléaire (IRSN), PSN-RES, SA2I, Cadarache, St Paul-Lez-Durance Cedex, 13115, France

## ABSTRACT

Cable fires are one of the main fire hazards present in nuclear power plants (NPPs). Therefore, as part of the OECD PRISME-2 project, cable tray fire tests were performed both in open atmosphere conditions and in a confined and mechanically-ventilated facility, called DIVA. These tests aim at showing the effects of a confined and ventilated environment on fire characteristics and consequences. This study deals with five fire tests which used halogenated (poly(vinyl chloride) or PVC) cable types. Two tests were carried out in open atmosphere and three tests in the DIVA facility. The latter used a ventilation renewal rate (VRR) of either 4 or 15 h<sup>-1</sup>. The confined and ventilated conditions reduced the mass loss rate and heat release rate compared with those obtained in open atmosphere. Furthermore, the three confined tests produced unburnt gases which ignited in the fire room. Two explosions were highlighted for the tests which used a VRR of 4 h<sup>-1</sup>. These explosions indeed led to fast flame propagations over the entire upper part of the fire room and steep overpressures of almost 150 hPa. The low-qualified PVC cables and the ventilation set-up used in this study strongly contributed to the occurrence of these explosions.

Keywords: cable tray fire; DIVA facility; explosion, ignition; PVC cable; unburnt hydrocarbons.

## NOMENCLATURE

AR	Adjacent room
CDG	Carbon dioxide generation
C	Soot (considered as pure carbon)
<i>c</i>	Specific heat (J.kg <sup>-1</sup> .K <sup>-1</sup> )
CO	Carbon monoxide
CO <sub>2</sub>	Carbon dioxide
C <sub>n</sub> H <sub>m</sub>	Unburnt hydrocarbons
CV	Confined and mechanically-ventilated
$\frac{d}{dt} m_j$	Mass variation rate of species <i>j</i> = CO <sub>2</sub> , CO or C in the FR or AR (g/s)
EHC	Effective heat of combustion (MJ/kg)
<i>E<sub>j</sub></i>	Energy produced by mass unit of generated species <i>j</i> = CO <sub>2</sub> , CO or C (MJ/kg)
FR	Fire room
HFFR	Halogen-free flame retardant
$\Delta H_{c,eff}$	Effective heat of combustion (MJ/kg)
HRR	Heat release rate (kW)
MLR, $\dot{m}$	Mass loss rate (g/s)
$\dot{m}_a$	Air mass flow rate at the inlet of the fire room (kg/s)
$\dot{m}_j^{out}$	Mass flow rate of species <i>j</i> = CO <sub>2</sub> , CO or C at the outlet of the AR (g/s)
NE	North-East
NW	North-West
O <sub>2</sub>	Oxygen

$\dot{Q}$	Heat release rate (kW)
$\dot{Q}_{CDG}$	Heat release rate assessed from the CDG calorimetry method (kW)
$\dot{Q}_{inst}$	Energy variation per unit of time within the FR and AR (kW)
$\dot{Q}_{out}$	Convective heat transfers through the inlet and outlet ducts of the ventilation network (kW)
$\dot{Q}_p$	Power law equation that fits best with the HRR time evolution of the fire growth stage (kW)
$\dot{Q}_{pyr}$	Energy per unit of time required for pyrolysis of fuel contained in the cables (kW)
$\dot{Q}_{thermal}$	Heat release rate assessed from the thermal method (kW)
$\dot{Q}_{walls}$	Heat transfers through the walls of both the FR and AR (kW)
PVC	Poly(vinyl chloride)
r	Stoichiometric mass fuel-to-air ratio (-)
SE	South-East
$t_1$	Fire growth characteristic time (s)
VRR	Ventilation renewal rate, i.e., number of changes of the room volume per hour ( $h^{-1}$ )

#### Greek characters

$\alpha$	Fire growth rate ( $kW/s^2$ )
$\phi$	Equivalence ratio (-)
$\lambda$	Thermal conductivity ( $W.m^{-1}.K^{-1}$ )
$\rho$	Density ( $kg.m^{-3}$ )
$\xi$	Combustion efficiency ratio (-)

#### Superscripts

-	Average
co	Confined conditions
o	Open atmosphere conditions

## 1 | INTRODUCTION

Several hundred kilometres of electric cables are present throughout nuclear power plants (NPPs). Power cables are used for instance in the process rooms for supplying electricity to the pumps, turbines, transformers or heaters, or in the switchgear room that contains numerous electric cabinets connected to multiple cable trays [1]. Furthermore, many cable trays containing both instrumentation and control cables are also found in the cable spreading room and in the main control room. Instrumentation cables are used for digital or analogic transmission for various types of transducers, while control cables can operate valves, relays or contactors.

A serious cable tray fire occurred at the Browns Ferry NPP in 1975 [2] resulting in the loss of the Unit One emergency core cooling system. Since then, many efforts have been made to enhance the prevention of cable tray fires in the most recent NPPs. For instance flame retardant materials have been used in cables. Nevertheless, the OECD FIRE Database [3] recorded nearly seventy fire events in NPPs involving electric cables between the late 1980s and the end of 2014. Cable tray fires and related consequences are therefore still a major issue for fire safety analyses in NPPs. Many cable tray fire experiments were carried out in the past and highlighted significant effect of the cable type [4], cable tray geometry [5], nearby ceiling [6] and support wall [7]-[8]. However, all these experiments were conducted in open atmosphere conditions and very few studies were performed in confined and mechanically-ventilated rooms [9], such as those found in NPPs. In contrast, many investigations, using hydrocarbon (Pretrel [10]-[11], Nasr [12], Melis [13], Lassus [14]), alcohol, polymethyl methacrylate (PMMA) or wood (Delichatsios [15]) as fuel, were conducted in mechanically-ventilated compartments. These fire tests showed a significant influence of the ventilation both on the combustion behaviour and species product formation. Compartment fires can indeed be classified as well-ventilated or under-

ventilated according to the ventilation conditions. Well-ventilated enclosure fires (Tewarson [16]) have an excess air supply compared with the quantity of air needed by the fuel and so they lead to a very low generation of unburnt gases. In contrast, for under-ventilated fires (Gottuk and Lattimer [17]), the air supply is too low and unburnt gases, such as carbon monoxide (CO) and unburnt pyrolysis gases, are produced. Such gas species may ignite in a confined and mechanically-ventilated compartment as highlighted in previous study [18]. Consequences of these ignitions, such as an overpressure or the occurrence of a secondary fire, are major issues for fire safety analyses in NPPs.

Therefore, as part of the OECD PRISME-2 project [19], cable tray fire tests were performed both in open atmosphere conditions and in a confined and mechanically-ventilated facility, called DIVA. These tests aim at showing the effects of a confined and ventilated environment on fire characteristics and consequences. The fire characteristics discussed are the mass loss rate (MLR), heat release rate (HRR), effective heat of combustion (EHC) and combustion efficiency ratio. The fire consequences studied in the DIVA facility are the fire room temperature, smoke concentration (carbon dioxide, unburnt hydrocarbon gases and soot), pressure and ventilation flow rates in particular. Moreover, partners of the PRISME-2 project proposed to use two halogenated (poly(vinyl chloride) or PVC) cable types and two halogen-free flame retardant (HFFR) cable types which can be found in their NPPs. This study only considers the tests performed using the PVC cable types while previous works [8],[20] have discussed the tests involving the two HFFR cable types.

This paper first gives a detailed description of the cable trays, the DIVA facility and the related instrumentation. Then, the main fire consequences in the DIVA facility are discussed, which leads to highlight several ignitions of unburnt hydrocarbon gases for each confined test. Next, the primary fire characteristics of the cable tray fire tests and ignitions of unburnt gases are assessed. The last part first proposes to discuss the effects of the confined and ventilated environment on the cable tray fires. For that purpose, the fire characteristics assessed in both confined and open atmosphere environment are compared. This analysis is completed by the classification of the confined and ventilated fires according to the assessment of the combustion efficiency ratio. Finally, this last section addresses the conditions that led to ignite the unburnt hydrocarbon gases and also highlights the fact that two ignitions can be considered as explosions.

## 2 | DESCRIPTION OF THE FIRE TESTS

The five cable tray fire tests of the OECD PRISME-2 project considered in this study are indicated in Table 1. The CT1 and CT3 tests were carried out in open atmosphere conditions and the CT2, CT4 and CT5 tests in confined and mechanically-ventilated conditions (DIVA facility). The CT1 to CT5 tests used a vertical stack of five horizontal ladder cable trays containing PVC cable types (Fig. 1). The CT1 and CT2 tests used a first PVC cable type, called cable A, while the CT3 to CT5 tests used a second type, named cable B (Table 1). These two cable types only meet the requirements of the international standard IEC 60332-1-2 test [21]<sup>1</sup> and can be thus considered as low-qualified electric cables. Finally, the CT2, CT4 and CT5 tests used a ventilation renewal rate (i.e., number of changes of the room volume per hour, VRR) of 4, 15 and 4 h<sup>-1</sup>, respectively.

### 2.1 | The cable trays

The cable trays were five horizontal ladder trays 3 m long and 0.45 m wide, with tray spacing of 0.3 m (Fig. 1). Each tray was filled with 49 cables A for the CT1 and CT2 tests and with 44 cables B for the CT3 to CT5 tests. The cables 2.4 m long were packed loosely along the five cable trays for all the tests, as illustrated in Fig. 2 for the CT2 test. This cable arrangement was also specified for nearly all the

---

<sup>1</sup> These two cable types do not meet the requirements of the C1 test of the French standard NF C 32-070 [22] (they failed this test) and they are not ranking according to the newly EUROCLASS standard (EN 13501-6 [23]) applicable in Europe. Indeed, cable B was manufactured in Japan. Moreover, cable A was produced in Europe but before 2012 when the EUROCLASS standard was not yet fully applicable.

horizontal cable tray experiments conducted as part of the CHRISTIFIRE project [5]. A loose arrangement of the cables can be considered as realistic. The constraints of setting up in real facilities can indeed prevent from an ordered arrangement of the electric cables. The electric cables A and B are shown in Fig. 3. The non-metallic materials (outer sheath, internal sheath and insulation) mainly contain plasticized PVC and mineral loads such as calcium carbonate ( $\text{CaCO}_3$ ). Phthalates are used as plasticizers in these cables. Other features of the cables A and B are provided in Table 2. Thermophysical properties of the outer sheath at  $20^\circ\text{C}$  are available for the cable B and are given in Table 3. The five ladder cable trays were placed against an insulated side wall which was 3 m long, 2.4 m high and 0.05 m deep (Fig. 1). Properties of this wall are given in [20]. A square gas burner ( $300 \times 300 \text{ mm}^2$ ), centred and located 0.2 m below the first tray (Fig. 1), was supplied with propane gas to ignite the cable trays. The burner provided a fire power of 80 kW for 1 minute 20 seconds during the CT1 and CT2 tests (cable A) and 2 minutes 26 seconds during the CT3 to CT5 tests (cable B). This power value of 80 kW was selected in order to ensure ignition of the cable trays regardless of the cable type and cable tray loading used in all the PRISME-2 cable tray fire tests [19]. The above durations were determined in open atmosphere conditions when the HRR of the cable tray fire reached 400 kW (without the gas burner contribution) [8]. For such an HRR value five times higher than the burner fire power, the cable trays were undoubtedly ignited and the previous durations were therefore considered as the times to ignition.

## 2.2 | Set-up of the rooms (DIVA facility and ventilation used)

This section details the configuration of the DIVA facility and ventilation used for the three confined CT2, CT4 and CT5 tests. This facility contains five rooms in total (Fig. 4). Firstly, the ground floor consists of 3 rooms (rooms 1 to 3) of similar size and arranged in a row separated by fire doors. Moreover, each room also provides access to a corridor (room 0 in the background of Fig. 4) through fire doors. A fifth room is located on the first floor (room 4). The bearing walls of these rooms, made of reinforced concrete, are 0.3 m thick and 4 m high. The ventilation system of the DIVA facility consists of two separate inlet and outlet circuits (in blue and red in Fig. 4, respectively) which are connected to each room. The multi-rooms DIVA facility can be representative of room configuration found in real NPPs as described in [1].

The CT2, CT4 and CT5 tests used rooms 1 and 2 of the DIVA facility as seen in Fig. 5 and Fig. 6. Room 1 was called the fire room (FR) since it contained the five cable trays. These cable trays were centred against the west wall (Fig. 6). Room 2 was named the adjacent room (AR). The features (dimension, position...) of the rooms, walls, inlet duct, outlet duct and five cable trays are given in Fig. 5 and Fig. 6. The FR and AR were linked through an open doorway which was 0.79 m wide and 2.17 m high. The ceiling of the FR was thermally protected by a double layer of 30 mm thick Rockwool panels while the ceiling of the AR was only protected by a single layer of the same insulated materials of 30 mm in thickness. Only one inlet duct was installed in the upper part of the FR and one outlet duct was positioned in the upper part of the AR. Flow directions at both the inlet and outlet are also indicated in Fig. 6. Initial VRR (before ignition) for all the volume occupied by both the FR and AR ( $240 \text{ m}^3$ ) was 4, 15 and  $4 \text{ h}^{-1}$  for the CT2, CT4 and CT5 tests, respectively. The corresponding ventilation volume flow rates at the inlet and outlet were thus initially equal to about 960, 3600 and  $960 \text{ m}^3/\text{h}$  for the CT2, CT4 and CT5 tests respectively.

## 2.3 | Instrumentation

This section presents the measurements discussed in this study. Nine thermocouples for measuring gas temperature were positioned in the North-West (NW), North-East (NE) and South-East (SE) corners of the FR along vertical trees (see the enlarged view in Fig. 7 (a) which shows, for instance, the thermocouples of the SE vertical tree). For the three trees, the spacing between the thermocouples was 0.5 m and the lowest and highest ones were located at 0.05 and 3.9 m from the floor, respectively. Only the temperature measurements at 1.05, 2.05, 3.05, 3.55 and 3.9 m are further shown in this work. Gas probes for continuous gas sampling were also located along the vertical tree in the SE corner at 0.7, 2.2

and 3.3 m from the floor (see the enlarged view in Fig. 7 (b) which only points out the gas probes). These probes were connected to gas analyzers (located outside the rooms) which measured the concentration of carbon dioxide (CO<sub>2</sub>), carbon monoxide (CO) and oxygen (O<sub>2</sub>) in the lower, mid and upper parts of the FR. An additional gas sampling probe was also fixed at the vertical tree in the SE corner at 3.2 m from the floor and was connected to a gas analyzer to measure the concentration of unburnt hydrocarbon gases (C<sub>n</sub>H<sub>m</sub>) in the upper part of the FR. In addition, concentration measurement of C<sub>n</sub>H<sub>m</sub> was also performed at the outlet of the AR. Furthermore, three smoke sampling probes were installed in the lower part of the FR and AR at 0.5 m from the floor and at the outlet duct of the AR. Each probe was connected to a bank of ten filters (BF) which measured the soot mass concentration in the three abovementioned locations. For each BF, ten smoke samplings for one minute duration were undertaken during different times of the test. These samplings led to soot deposits on each filters. The pressure in the FR, volume flow rate at the inlet and one heat flux measurement, positioned above the cable trays at 0.7 m from the ceiling of the FR, named HF (Fig. 8), are also discussed in this study. Finally, the mass loss was recorded from two electronic scales. These scales were placed in thermally insulated and metallic boxes and positioned below the supporting device of the cable trays (Fig. 8).

### 3 | RESULTS AND DISCUSSION

#### 3.1 | Fire spread over the cable trays

An illustration of the fire spread over the five horizontal ladder cable trays is given in Fig. 9 for the CT2 test. The fire quickly spread vertically between the trays and the top tray was quickly involved in the fire 30 s after ignition (Fig. 9 (a)), and then fire spread horizontally (Fig. 9 (b) and (c)). At the same time, smoke also rapidly filled up the FR as seen in Fig. 9 (c) to (e) which indicate pictures of the cable trays at  $t = 2, 3$  and 4 min, respectively. Moreover, Fig. 10 and Fig. 11 show the cable trays before and after the CT4 and CT5 tests, respectively. Fig. 9 (f) and Fig. 10 (b) first show that fire spread to the ends of the five cable trays for the CT2 and CT4 tests (VRR of 4 and 15 h<sup>-1</sup>, respectively). Identical outcome was obtained for the CT1 and CT3 fire tests which were preliminarily conducted in open atmosphere conditions [8]. However, for the CT5 test (VRR of 4 h<sup>-1</sup>), Fig. 11 (b) demonstrates that fire reached the five cable trays but it did not propagate up to the extremities of all the cable trays, especially for the lower cable trays. Therefore, a VRR of 4 h<sup>-1</sup> limited the fire spread over the five cable trays containing the cable B (i.e., CT5 test) but not over those filled with the cable A (i.e., CT2 test).

#### 3.2 | Fire consequences in the fire room (FR)

Fig. 12 to Fig. 14 point out the gas temperatures measured in the NW, NE and SE corners of the FR for the three CT2, CT4 and CT5 tests, respectively. These figures first show an increase of the gas temperatures for the three tests due to the growth of the cable tray fires. Then, during the decay fire stages of each test, two faster time evolutions of the temperatures are highlighted and lead to the temperature peaks (1) to (6) exceeding 600°C in the upper half-part of the FR. Flames are identified at location where temperatures are measured in excess of 600 °C. Drysdale previously used this as an indicator of flames [24]. In addition, Fig. 15 and Fig. 16 give the respective CO<sub>2</sub> and O<sub>2</sub> concentrations in the FR for the CT2, CT4 and CT5 tests. These figures indicate that the abovementioned temperature peaks (1) to (6) match with the sudden and significant variations (1) to (6) of both CO<sub>2</sub> and O<sub>2</sub> concentrations in the upper half-part of the FR. These simultaneous temperature and concentrations variations clearly reveal the fact that gas ignitions occurred twice for each test in the upper part of the FR during the decay fire stage. Moreover, Fig. 17 shows the concentration of the unburnt hydrocarbon gases (C<sub>n</sub>H<sub>m</sub>) measured in the upper part of the FR (i.e., 3.2 m high from the floor) as well as at the outlet of the AR for the CT2, CT4 and CT5 tests. This figure and Fig. 12 to Fig. 16 indicate that the decreases (1) to (6) of C<sub>n</sub>H<sub>m</sub> concentration<sup>2</sup> correspond with previous variations (1) to (6) of gas

---

<sup>2</sup> For the CT2 test, the decrease (2) of C<sub>n</sub>H<sub>m</sub> concentration in the FR was not observed since the related analyzer

temperature as well as CO<sub>2</sub> and O<sub>2</sub> concentrations. This undoubtedly showed that C<sub>n</sub>H<sub>m</sub> ignited twice in the upper half-part of the FR for each of the three tests.

Furthermore, Fig. 18 indicates that maximal soot mass concentrations were measured in the range 3-4 g/m<sup>3</sup> in both the FR and AR for the three CT2, CT4 and CT5 tests. In addition, Fig. 19 points out the same measurements carried out during two additional cable tray fire tests which were also conducted in the DIVA facility as part of the OECD PRISME-2 project [20]. All the characteristics of these tests (cable tray geometry, room set-up, VRR...) were identical to those of the CT2, CT4 and CT5 tests, except for the cable type. They indeed used one HFFR cable type, as earlier mentioned in the introduction, and specified in detail in [20]. Fig. 18 and Fig. 19 indicate that the soot mass concentrations in the FR and AR are significantly lower for the tests which used the HFFR cable type compared with the CT2, CT4 and CT5 tests which involved the PVC cable types. This outcome was expected since the HFFR cable<sup>3</sup> [20] satisfies the requirements of IEC 61034-2 [25] unlike the PVC cable types.

Finally, Fig. 20 and Fig. 21 point out the pressure in the FR and AR, respectively, and the volume flow rate at the inlet of the FR, for the three confined CT tests. These figures show that the higher pressure peaks (1), (2) and (6) led to strong reversals (1), (2) and (6) of the volume flow rates at the inlet of the FR for CT2 and CT5 tests. This last outcome thus indicates that smoke exited from the FR to the inlet ventilation circuit of the DIVA facility. Table 4 provides the main consequences of the unburnt gases ignitions (1) to (6) such as the pressure peaks, the related minimal flow rates at the inlet (as well as the nominal values) and the C<sub>n</sub>H<sub>m</sub> combustion zone. This combustion zone is the region involved by the combustion of the unburnt gases. It was estimated according to the locations of temperature measurements higher than 600°C in the NW, NE and SE corners at the peaks (1) to (6) (Fig. 12 to Fig. 14, respectively). Table 4 shows that the C<sub>n</sub>H<sub>m</sub> ignitions (1), (2) and (6) involved a large combustion zone in the upper part of the FR and led to steep pressure peaks in the range 70-150 hPa as well as important reversals of the volume flow rate at the inlet (in the range 3000-5000 m<sup>3</sup>/h from the FR to the inlet ventilation circuit). In contrast, the C<sub>n</sub>H<sub>m</sub> ignitions (3), (4) and (5) involved a limited combustion zone (in the NW corner of the FR, under the ceiling) and led to clearly lower consequences than the above ignitions. Consequently, the C<sub>n</sub>H<sub>m</sub> ignitions (1), (2) and (6) are considered as severe ignitions compared with the other C<sub>n</sub>H<sub>m</sub> ignitions (3), (4) and (5).

### 3.3 | Characteristics of the cable tray fires and C<sub>n</sub>H<sub>m</sub> ignitions

#### 3.3.1 | Mass loss rate

Fig. 22 provides the mass loss rate (MLR or  $\dot{m}$ ) of the cable trays for the CT2, CT4 and CT5 tests, obtained from time derivation of the mass loss. Marks (1) and (2) in Fig. 22 (a) and mark (6) in Fig. 22 (c) reveal sharp increases in MLR of the CT2 and CT5 tests, respectively. These increases were likely caused by the radiation effect related to the severe C<sub>n</sub>H<sub>m</sub> ignitions (1), (2) and (6) as seen in Fig. 23 (a) and (c). These figures indeed indicate corresponding heat flux peaks (1), (2) and (6) measured in the range 55-70 kW/m<sup>2</sup> at a height of 3.3 m (see HF in Fig. 8). A feed-back effect on the MLR is thus likely shown for the CT2 and CT5 tests. In contrast, for the CT4 test, this radiation effect is not visible for the MLR (Fig. 22 (b)) since the heat flux peaks (3) and (4), related to the two C<sub>n</sub>H<sub>m</sub> ignitions (3) and (4), were lower (maximal value of 40 kW/m<sup>2</sup>, Fig. 23 (b)).

---

malfunctioned before (i.e., from  $t = 645$  s as seen in Fig. 17 (a)). Nevertheless, since C<sub>n</sub>H<sub>m</sub> concentration at the outlet of the AR decreased at the event (2) (Fig. 17 (a)), it is thus supposed that C<sub>n</sub>H<sub>m</sub> concentration in the FR also dropped at the same time. The same analyzer also malfunctioned for the CT4 test from  $t = 1270$  s (Fig. 17 (b)). These malfunctions would very likely be caused by the overpressures which followed the C<sub>n</sub>H<sub>m</sub> ignitions, as further discussed.

<sup>3</sup> In the same way as for the two PVC cable types studied in this work, this HFFR cable, as specified in [20], was not classified according to the newly applicable EUROCLASS standard in Europe (EN 13501-6 [23]). Indeed, this cable was produced in Europe before 2012 when the EUROCLASS standard was not yet fully applicable.

### 3.3.2 | Heat release rate

Heat release rates (HRR or  $\dot{Q}$ ) for the cable tray fire tests in the DIVA facility were determined from the thermal method and the carbon dioxide generation (CDG) calorimetry method. The former method was developed by Coutin *et al.* [26] for assessing the HRR of a cabinet fire, by establishing an energy balance in a single fire room. In this work, the energy balance was carried out inside both the FR and AR (Fig. 6) and the heat released by the fire was mainly distributed in four main parts<sup>4</sup>:

- energy per unit of time required for pyrolysis of fuel contained in the electric cables ( $\dot{Q}_{pyr}$ ),
- heat transfers through the walls of both the FR and AR ( $\dot{Q}_{walls}$ ),
- energy variation per unit of time within the FR and AR ( $\dot{Q}_{inst}$ ),
- convective heat transfers through inlet and outlet ducts of the ventilation network ( $\dot{Q}_{out}$ ).

The HRR from the thermal method ( $\dot{Q}_{thermal}$ ) was thus assessed using the following relationship:

$$\dot{Q}_{thermal} = \dot{Q}_{pyr} + \dot{Q}_{walls} + \dot{Q}_{inst} + \dot{Q}_{out} \quad (1)$$

Moreover, the HRR of the fire can be also estimated with the CDG calorimetry method which was first proposed by Pretrel *et al.* [27] for fires in a multi-rooms facility. This approach also relies on mass balances of CO<sub>2</sub>, CO and soot carried out in the rooms of such a facility. This method was applied to the CT2, CT4 and CT5 tests, as was the case for previous cable tray fire tests [20]. The HRR was thus assessed from the CDG method ( $\dot{Q}_{CDG}$ ) and mass balances of gas species conducted in all the volumes involving the FR and AR. The HRR formulation is given as follows:

$$\begin{aligned} \dot{Q}_{CDG} &= E_{CO_2} \left[ \dot{m}_{CO_2}^{out} + \frac{d}{dt} m_{CO_2}^{FR} + \frac{d}{dt} m_{CO_2}^{AR} \right] \\ \dot{Q}_{CDG} &= E_{CO_2} \left[ \dot{m}_{CO_2}^{out} + \frac{d}{dt} m_{CO_2}^{FR} + \frac{d}{dt} m_{CO_2}^{AR} \right] \\ &+ E_{CO} \left[ \dot{m}_{CO}^{out} + \frac{d}{dt} m_{CO}^{FR} + \frac{d}{dt} m_{CO}^{AR} \right] + E_C \left[ \dot{m}_C^{out} + \frac{d}{dt} m_C^{FR} + \frac{d}{dt} m_C^{AR} \right] \end{aligned} \quad (2)$$

Where  $E_j$  is the energy produced by mass unit of generated species  $j = \text{CO}_2, \text{CO}$  or  $\text{C}$  (i.e., soot) (MJ/kg),  $\dot{m}_j^{out}$  is the mass flow rate of species  $j = \text{CO}_2, \text{CO}$  or  $\text{C}$  at the outlet of AR (g/s) and  $\frac{d}{dt} m_j^{FR}$  and  $\frac{d}{dt} m_j^{AR}$  are the mass variation rates of species  $j = \text{CO}_2, \text{CO}$  or  $\text{C}$  in the FR and AR, respectively (g/s). The average  $E_{CO_2}$  and  $E_{CO}$  considered are 13.3 and 11.1 MJ/kg, respectively [28] and 15.8 MJ/kg for  $E_C$  [27].

For each fire test, HRR evaluations were thus carried out from the previous thermal and CDG calorimetry methods, and they are shown in Fig. 24. Considering that the thermal method can underestimate the HRR by about 15% due to heat sinks not considered in the thermal method [26] and that the CDG method can generally overestimate the HRR, as already highlighted in [20] and [29], the two evaluations above can be considered to be rather consistent. These considerations also lead to assess the final HRR ( $\dot{Q}$ ) as the average of the two previous HRR assessments:

$$\dot{Q} = \frac{\dot{Q}_{thermal} + \dot{Q}_{CDG}}{2} \quad (3)$$

<sup>4</sup> Coutin *et al.* [26] also considered the contribution of thermal inertia of the metallic structures of the cabinet in the HRR. For the five ladder-type trays considered in this study this contribution may be neglected compared with the other contributions discussed hereafter.



Fig. 25 therefore gives the final HRR assessed from Eq. (3) for the CT2, CT4 and CT5 tests. Given that  $\dot{Q}_{thermal}$  can generally underestimate  $\dot{Q}$  while  $\dot{Q}_{CDG}$  tends to over-estimate it, as above discussed, it is thus assumed that  $\dot{Q}$  falls in the interval  $\left[ \dot{Q} - \left| \frac{\dot{Q}_{CDG} - \dot{Q}_{thermal}}{2} \right|; \dot{Q} + \left| \frac{\dot{Q}_{CDG} - \dot{Q}_{thermal}}{2} \right| \right]$  at every time with a proper degree of confidence.  $\left| \frac{\dot{Q}_{CDG} - \dot{Q}_{thermal}}{2} \right|$  is actually the standard deviation or uncertainty<sup>5</sup> ( $u$ ) at every time of  $\dot{Q}$  estimated from the two HRR measurements (i.e.,  $\dot{Q}_{CDG}$  and  $\dot{Q}_{thermal}$ , see Fig. 24). The relative uncertainty  $\tilde{u}$  of  $\dot{Q}$  is then evaluated as follows:

$$\tilde{u} = \frac{u}{\dot{Q}} \quad (4)$$

Average of  $\tilde{u}$  is finally assessed over time intervals of [0 s; 1500 s] for CT2, [0 s; 2500 s] for CT4 and [0 s; 2000 s] for CT5, which gives 29, 15 and 27 %, respectively. In contrast, for time beyond previous time intervals, values  $\dot{Q}$  are low (Fig. 25), which leads to high values of  $\tilde{u}$ . In this case, it is more suitable to assess (absolute) uncertainty  $u$  of  $\dot{Q}$ . Therefore, for time intervals of [1500 s; 2000 s] for CT2, [2500 s; 3000 s] for CT4 and [2000 s; 3000 s] for CT5, average of  $u$  is assessed lower than 50 kW for all the tests.

Fig. 25 first shows the growth of the cable tray fire when the fire spread over the five cable trays and then a rather steady fire stage for the CT2 and CT4 tests only. This figure finally shows the fire decay stage for the three tests which highlights the HRR peaks (1) to (6). These peaks, which are related with the  $C_nH_m$  ignitions (1) to (6), confirm that these ignitions occurred during the decay fire stage of the three tests.

Furthermore, Fig. 25 (a) and (c) also indicate that the HRR peak due to the cable tray fire is clearly higher for the CT2 test and the cable A (0.98 MW) than for the CT5 test and the cable B (0.57 MW). These two tests involved a VRR of 4 h<sup>-1</sup>. This result corroborates the fact that higher MLR peak was measured for the CT2 test (100 g/s) than for the CT5 test (62 g/s), as previously seen in Fig. 22 (a) and (c). So regarding the MLR and HRR, the cable trays filled with the cable B have significantly better fire performances than those containing cable A, even if the two cables meet the same requirements (IEC 60332-1-2 test, see section 2).

### 3.3.3 | Growth rate

It is commonly assumed that the growth of a fire may be described by the following power law equation [31]:

$$\dot{Q}_p(t) = \alpha \cdot (t - t_o)^2 \quad (5)$$

Where  $\dot{Q}_p(t)$  is given by the above power law equation that fits best with the HRR time evolution of the fire growth stage (kW),  $\alpha$  is the fire growth rate (kW/s<sup>2</sup>),  $t$  is the time (s) and  $t_o$  is the starting time of  $\dot{Q}_p(t)$  (s). In addition,  $t_1$ , the fire growth characteristic time (s), is defined as the time necessary after  $t_o$  to reach a HRR of 1000 kW (s).  $t_1$  is estimated as follows:

$$t_1 = \sqrt{\frac{1000}{\alpha}} \quad (6)$$

It is also proposed to assess the growth rate of the HRR generated by the ignitions of the unburnt gases (1) to (6) in the same way as for the cable tray fires, as discussed above. Fig. 26 to Fig. 28 give enlarged views of the growth stage of the HRR for both the cable tray fire and  $C_nH_m$  ignitions, for the CT2, CT4

<sup>5</sup> As specified in [30].

and CT5 tests, respectively. Table 5 also reports the growth rates,  $\alpha$ , the growth characteristic times,  $t_1$ , and the HRR peaks, for the three cable tray fires and  $C_nH_m$  ignitions (1) to (6) from these tests. This table indicates that the growth rates of the HRR produced by the severe  $C_nH_m$  ignitions (1), (2) and (6) ( $\alpha$  in the range 5.5-35 kW/s<sup>2</sup>) are significantly higher than those for both the  $C_nH_m$  ignitions (3), (4) and (5) and cable tray fires ( $\alpha$  in the ranges 0.08-0.23 kW/s<sup>2</sup> and 0.022-0.19 kW/s<sup>2</sup> respectively). This outcome implies that flame propagation in the upper half-part of the FR for the severe  $C_nH_m$  ignitions (1), (2) and (6) was significantly faster than that for the other  $C_nH_m$  ignitions (3), (4) and (5) and also than the fire propagation over the five cable trays. Such outcomes are also illustrated by the assessment of  $t_1$  (Table 5). Indeed, it took about 5 to 13 s for the severe  $C_nH_m$  ignitions (1), (2) and (6) to generate a HRR of 1 MW while the same value of HRR was reached from 66 to 112 s and 79 to 213 s for the other  $C_nH_m$  ignitions (3), (4) and (5) and cable tray fires, respectively. It should be noted that only the HRR determined from the thermal method (Fig. 24 (a) and (c)) was used for the assessment of  $\alpha$  and  $t_1$  for the severe  $C_nH_m$  ignitions (Fig. 26 (b) and (c) and Fig. 28 (c)). Indeed, the key sensors used for this method such as the heat flux sensors have faster response-time than gas analysers used for the CDG method. This implies that the thermal method better estimates the fast time evolution of the HRR for the severe ignitions than the CDG method.

Finally, the HRR peaks produced by the severe  $C_nH_m$  ignitions (1), (2) and (6) were also deduced from the HRR determined from the thermal method as argued above. These last ones are thus in the range 0.5-1.75 MW while those produced by the other  $C_nH_m$  ignitions (3), (4) and (5) vary from 0.3 to 0.5 MW (Table 5).

### 3.3.4 | Effective heat of combustion

The combustion behaviour of the cable tray fires can be first characterized by the effective heat of combustion ( $EHC$  or  $\Delta H_{c,eff}$ ) defined as the ratio of HRR ( $\dot{Q}$ ) to MLR ( $\dot{m}$ ) [32]:

$$\Delta H_{c,eff} = \frac{\dot{Q}}{\dot{m}} \quad (7)$$

EHC was evaluated from Eq. (7) for the CT2, CT4 and CT5 tests and then averaged over time intervals corresponding to MLR values higher than 20% of the peak MLR. Such a method, as done in [33], leads to minimization in EHC uncertainty. Indeed, this assessment therefore does not consider the low values of the MLR at the early and late fire stages, which can be affected by significant uncertainty. The average EHC (or  $\overline{\Delta H_{c,eff}}$ ) was thus assessed at 13, 12.5 and 8 MJ/kg, over time intervals of [40 s; 810 s] for the CT2 test, [20 s; 1770 s] for the CT4 test and [30 s; 1730 s] for the CT5 test, respectively.

## 3.4 | Effects of the confined and ventilated conditions

This section first proposes to discuss the effects of the confined and mechanically-ventilated conditions on the cable tray fires of the CT2, CT4 and CT5 tests. For this purpose, a comparison with the CT1 and CT3 fire tests performed in open atmosphere conditions [8] is made; Table 6 summarizes the main fire characteristics. This comparative analysis is completed by the assessment of the combustion efficiency ratio between the confined and open fires, as presented hereafter. Finally, the last part of this section addresses the conditions that led to ignite the unburnt gases.

### 3.4.1 | Combustion efficiency ratio

To compare the combustion efficiency of the cable tray fires conducted in confined conditions and open atmosphere conditions, the combustion efficiency ratio ( $\xi$ ) may be assessed according to [20],[32] as follows:

$$\xi = \frac{\overline{\Delta H_{c,eff}^{co}}}{\overline{\Delta H_{c,eff}^o}} \quad (8)$$

Where  $\overline{\Delta H_{c,eff}^{co}}$  and  $\overline{\Delta H_{c,eff}^o}$  are the average EHC of the cable tray fires conducted in confined conditions and open atmosphere conditions respectively. It is stated from [20],[32] that:

- for  $\xi < 1$ , the cable tray fire in confined conditions has a lower combustion efficiency than in open atmosphere conditions (i.e., in well-ventilated conditions) and can thus be classified as an under-ventilated fire or ventilation-controlled fire,
- for  $\xi \sim 1$ , the cable tray fire in confined conditions has similar combustion efficiency than in open atmosphere conditions and can be therefore considered as an well-ventilated fire or fuel-controlled fire.

However, it should be noted that the global equivalence ratio,  $\phi$ , is commonly used to classify fire. For fire compartment,  $\phi$ , can be assessed, according to Gottuk and Lattimer [17], as follows :

$$\phi = \frac{\dot{m}/\dot{m}_a}{r} \quad (9)$$

Where  $\dot{m}_a$  is the air mass flow rate at the inlet of the fire compartment (kg/s) and  $r$  is the stoichiometric fuel-to-air ratio. It is widely agreed that fire is well-ventilated when the related  $\phi$  is lower than 1, otherwise the fire is under-ventilated [17]. Given the test set-up used for the CT2, CT4 and CT5 tests (Fig. 5), it is supposed that only a fraction of the inlet air mass flow rate ( $\dot{m}_a$ ) reached the fuel (i.e., the cable trays). Other fraction of  $\dot{m}_a$  can indeed enter either in the AR through the doorway (Fig. 5) or can mix with the unburnt gases and combustion gas products in the upper part of the FR. Previous work [1] also mentioned that in fire compartment not all of the air supplied by the ventilation system does reach the fire, especially for ceiling-mounted supply ducts. So, for the CT2, CT4 and CT5 tests, considering the total inlet air mass flow rate ( $\dot{m}_a$ ) in Eq. (7) can lead to assess  $\phi$  lower than 1 while the related cable tray fire can be actually under-ventilated. Additional illustration of above discussion is found in [18] that studied hydrocarbon fire (dodecane and heptane) in a reduced-scale confined and mechanically-ventilated enclosure. The authors of this study indeed stated under-ventilated fires that could be characterized by  $\phi$  lower than 1 (they specified under-ventilated fires for  $0.7 \leq \phi < 1.5$ ). For the current work, the use of the combustion efficiency ratio,  $\xi$  (Eq. ((8)), to classify the fire was therefore preferred. This last one was indeed assessed from fire characteristics such as the heat release rate which strongly depends on the air (i.e., oxygen) mass flow rate consumed by the fuel [27],[32]. This leads to a proper fire classification regardless of the test configuration. In contrast, as commented above, the global equivalence ratio,  $\phi$ , can overestimate the amount of oxygen available for fuel when considering the inlet air mass flow rate,  $\dot{m}_a$ , in Eq. (9), which can thus lead to underestimate its evaluation.

### 3.4.2 | Fire classification

Fig. 29 and Fig. 30 show the MLR and HRR for the CT1/CT2 tests (cable A) and the CT3 to CT5 tests (cable B) respectively. These figures first indicate that both the MLR and HRR of the confined and mechanically-ventilated tests initially grew in a similar way as the fires preliminarily conducted in open atmosphere conditions [8]. Such an outcome thus reveals no oxygen limitation during the early fire stages. Then, both the MLR and HRR growths for the confined and ventilated cable tray fires suddenly stopped due to an oxygen concentration decrease in the FR (Fig. 16). Consequently, the peaks of both the MLR and HRR are reduced compared with those obtained for the related fire tests performed in open atmosphere conditions. The ratios of the MLR peaks between CT1 and CT2, CT3 and CT4 as well as CT3 and CT5 are about 1.6, 3.0 and 2.8 respectively (Table 6). The ratios of the HRR peaks between

CT1 and CT2, CT3 and CT4 as well as CT3 and CT5 are about 3.3, 3.6 and 4.7 respectively (Table 6). These last outcomes indicate that for the three confined and ventilated cable tray fires, the HRR reduction was higher than for the MLR. This implies that a fraction of pyrolysis gases was not involved in the cable tray fire and thus increased the amount of unburnt gases accumulated under the ceiling of the FR or exited to the AR. This outcome is confirmed hereafter through the assessment of the combustion efficiency ratio.

The ratio of the combustion efficiencies of the CT2 and CT1 cable tray fires,  $\xi_1$ , is evaluated from Eq. (8) with the corresponding average EHC given in Table 6. So  $\xi_1$  gives 0.58.  $\xi_2$  of the CT4 and CT3 cable tray fires and  $\xi_3$  of the CT5 and CT3 cable tray fires are evaluated in the same way as for  $\xi_1$  and thus give 0.74 and 0.47, respectively. The confined and mechanically-ventilated cable tray fires of the CT2, CT4 and CT5 tests are therefore classified as under-ventilated fires since  $\xi < 1$  (section 3.4.1).

### 3.4.3 | Conditions leading to ignite the unburnt hydrocarbon gases ( $C_nH_m$ )

This section proposes to discuss the conditions leading to the ignitions of the unburnt hydrocarbon gases for all the confined tests and also why the two ignition types (either severe or not) were observed. First, the three under-ventilated CT2, CT4 and CT5 cable tray fires ( $\xi < 1$ ) released unburnt hydrocarbon gases which accumulated under the ceiling of the FR since there was no outlet duct in this room, as specified in section 2.2. In addition,  $C_nH_m$  mixed with the incoming air from the inlet located in the upper part of the FR (Fig. 5). During the formation of this premixed medium, the cable tray fire was still burning for the three tests (Fig. 25). So, once the premixed gas mixture reached the flammable range, it was very likely ignited by the burning cable trays (its top was located at about 2.2 m from the floor, see Fig. 5). Next,  $C_nH_m$  combustion involved either a limited or a large volume located in the upper part of the FR (Table 4). One of the plausible explanations of this difference would be due to the higher  $C_nH_m$  concentrations obtained before the severe ignitions (1), (2) and (6) than before the other ones (3), (4) and (5). This would indeed increase the premixed gas mixture zone where the flammable range was reached. This observation is notably confirmed when comparing  $C_nH_m$  concentrations for the CT4 and CT5 tests which used the same cable B but a distinct VRR of 15 and 4  $h^{-1}$ , respectively. The  $C_nH_m$  concentrations were indeed higher before the severe ignition (6) (Fig. 17 (c)) than before the other ignitions (3), (4) and (5) (Fig. 17 (b) and (c), respectively). In summary, severe  $C_nH_m$  ignitions occurred for the lower VRR (4  $h^{-1}$ ) (i.e., a lower  $\xi$ , as seen in Table 6) and especially during the fire decay stage. Moreover, the ventilation set-up specified for these tests (no outlet duct in the FR and an air inlet located in the upper part of the FR) also contributed to the occurrence of the  $C_nH_m$  ignitions.

### 3.4.4 | Explosions

Croft [34], Dobashi [35] and Zalosh [36] stated that a gas explosion can be characterized by a fast flame propagation through a premixed gas mixture of combustible gases and air. In addition, these authors also indicated that such explosion may result in a fast increase of the pressure when a confinement prevented the unrestrained expansion of the combustion products. Croft specified that the related overpressures could be in the range 50-100 hPa or higher and that the time to flashover could be of few seconds according to the enclosure size. Therefore, the severe ignitions (1) and (6) can be considered as explosions. These ignitions are indeed characterized by a fast flame propagation in the entire upper half-part of the FR where the premixed medium was formed, HRR peaks exceeded 1 MW (i.e., flashover) in few seconds and steep overpressures of almost 150 hPa (see Table 4 and Table 5). Otherwise, for the third severe ignition (2), its classification as an explosion is not as obvious as previously. Indeed, even if the related overpressure was around 70 hPa, the fast flame propagation did not involve all the upper half-part of the FR and the HRR peak was limited to about 0.5 MW (see Table 4 and Table 5). So this study only considers the severe ignitions (1) and (6) as explosions.

## 4 | CONCLUSION

As part of the OECD PRISME-2 project, cable tray fire tests were performed both in open atmosphere conditions and in a confined and mechanically-ventilated facility, called DIVA. These tests aim at showing the effects of a confined and ventilated environment on fire characteristics and consequences. This study deals with five cable tray (CT) fire tests which used two halogenated (poly(vinyl chloride) or PVC) cable types. Two CT tests, namely CT1 and CT3, were carried out in open atmosphere conditions and three tests, CT2, CT4 and CT5, were performed in the DIVA facility. The five CT1 to CT5 tests used a vertical stack of five horizontal ladder cable trays supported by a wall. The CT1 and CT2 tests used a first PVC cable type, called cable A, while the CT3 to CT5 tests used a second type, named cable B. These two cable types only meet the requirements of the international standard IEC 60332-1-2 test and can be thus considered as low-qualified electric cables. Moreover, the CT2, CT4 and CT5 tests used a ventilation renewal rate (i.e., the number of changes of the room volume per hour, VRR) of 4, 15 and 4 h<sup>-1</sup>, respectively. These tests used two rooms of the DIVA facility; a fire room (FR) that contained the five cable trays and an adjacent room (AR). Only one inlet duct was installed in the upper part of the FR and one outlet duct was positioned in the upper part of the AR.

Fire spread to the ends of the five cable trays for all the CT fire tests conducted in open and confined conditions, except for the confined CT5 test (VRR of 4 h<sup>-1</sup>). Therefore, the decrease of the VRR (from 15 to 4 h<sup>-1</sup>) can limit the fire spread over the cable trays in confined conditions.

The confined and mechanically-ventilated conditions reduced the mass loss rate (MLR) and heat release rate (HRR) compared with those obtained in open atmosphere conditions. Moreover, this reduction is higher for the HRR than for the MLR. The three confined cable tray fire tests are indeed under-ventilated fires, as confirmed by the assessment of the combustion efficiency ratio. They thus released unburnt hydrocarbon gases which accumulated in the FR and mixed with the incoming air from the inlet located in the upper part of the FR. The premixed medium then ignited twice in the upper half-part of the FR for each fire test. The gas mixture was very likely ignited by the residual cable tray fire. Severe ignitions of unburnt gases were highlighted for the two less ventilated confined tests (VRR of 4 h<sup>-1</sup>). Two of these severe ignitions can be considered as explosions and occurred during the CT2 and CT5 tests. These explosions are indeed characterized by fast flame propagations over the entire upper half-part of the FR, HRR peaks exceeded 1 MW in few seconds, steep overpressures of almost 150 hPa. Therefore, the use of low-qualified PVC cables, a VRR of 4 h<sup>-1</sup> and the set-up of both inlet and outlet as specified in this study, significantly contributed to the occurrence of these explosions.

## ACKNOWLEDGMENT

This work was performed by IRSN in the framework of the OECD PRISME-2 project with the support of the partners: ENGIE and Bel V (Belgium), CNSC (Canada), VTT (Finland), DGA and EDF (France), GRS (Germany), NRA and CRIEPI (Japan), CSN (Spain), SSM (Sweden) and ONR, an agency of the HSE (United Kingdom).

## REFERENCES

1. U.S. NRC and EPRI (2007), Verification and validation of selected fire models for nuclear power plant applications, NUREG-1824, U.S. Nuclear Regulatory Commission, Washington, DC
2. U.S. NRC (1975), Cable Fire at Browns Ferry Nuclear Power Station, NRC Bulletin BL-75-04, U.S. Nuclear Regulatory Commission, Washington, DC
3. Organisation for Economic Co-operation and Development (OECD) Nuclear Energy Agency (NEA), Committee on the Safety of Nuclear Installations (CSNI): "OECD FIRE Database, Version: OECD FIRE DB 2014:2", Paris, France (2016), proprietary, for members only
4. Grayson, S. J., Van Hees, P., Green, A.M., Breulet, H., Vercellotti, U., 2001, Assessing the Fire Performance of Electric Cables (FIPEC), Fire and Materials, 25, p49-60
5. McGrattan, K., Lock, A., Marsh, N., Nyden, M., Bareham, S., Price, M., Morgan, A.B., Galaska, M., Schenck, K., Stroup, D., 2012, Cable Heat Release, Ignition, and Spread in Tray Installations

- During Fire (CHRISTIFIRE). Volume 1: Horizontal Trays, NUREG/CR-7010, U.S.NRC
6. McGrattan, K., Bereham, S., 2013, Cable Heat Release, Ignition, and Spread in Tray Installations During Fire (CHRISTIFIRE). Phase 2: Vertical Shafts and Corridors, NUREG/CR-7010, Vol. 2, U.S.NRC.
  7. Passalacqua, R., Cortes, P., Taylor, N., Beltran, D., Zavaleta, P., Charbaut, S., 2013, Experimental characterisation of ITER electric cables in postulated fire scenarios, *Fusion Engineering and Design*, 88, p2650-2654
  8. Zavaleta, P., Charbaut, S., Basso, G., Audouin, L., 2013, Multiple Horizontal Cable Tray Fire in Open Atmosphere, Thirteenth international conference of the Fire and Materials, San Francisco, USA, p57-68.
  9. Keski-Rahkonen, O., Mangs, J., Bertrand, R., Röwekamp, M., Fire induced damage to electrical cables and fire growth on cables, EUROSAFE 2002, Forum for nuclear safety, Berlin
  10. Pretrel, H., Le Saux, W., 2005, Experimental study of the burning rate behaviour of a pool fire in confined and ventilated compartment, Post-SMIRT18, Vienna
  11. Pretrel, H., Querre, P., Forestier, M., 2005, Experimental study of burning rate behaviour in confined and ventilated fire compartments, in: *Proceedings of the 8th International Symposium on Fire Safety*, Beijing
  12. Nasr, A., Suard, S., El-Rabii, H., Gay, L., Garo, J.P., 2011, Fuel Mass-Loss Rate Determination in a Confined and Mechanically Ventilated Compartment Fire Using a Global Approach, *Combustion Science and Technology*, 183:12, p1342-1359
  13. Melis, S., Audouin, L., Effects of vitiation on the heat release rate in mechanically-ventilated compartment fires. In: *Fire Safety Science, Proceedings of the Ninth International Symposium*, 9, International Association
  14. Lassus, J., Courty, L., Garo, J.P., Studer E., Jourda, P., Aine, P., 2014, Ventilation effects in confined and mechanically ventilated fires, *International Journal of Thermal Sciences*, 75, p87-94.
  15. Delichatsios, M.A., Silcock, G.W.H., Liu, X., Delichatsios, M., Lee, Y., 2004, Mass pyrolysis rates and excess pyrolysate in fully developed enclosure fires, *Fire Safety Journal*, 39, p1-21
  16. Tewarson, A., Jiang, F.H., Morikawa, T., 1993, Ventilation-Controlled Combustion of Polymers, *Combustion And Flame*, 95, p151-169
  17. Gottuk, D.T., Lattimer, B.Y., 2002, Effect of Combustion Conditions on Species Production, SFPE handbook of Fire Protection Engineering 2002, ISBN:087765-451-4, Third edition, Section two, Chapter 5
  18. Magnognou, B., Garo, J.P., Coudour, B., Wang, H.Y., Risk analysis of unburnt gas ignition in an exhaust system connected to a confined and mechanically ventilated enclosure fire, IAFSS 12th Symposium 2017, *Fire Safety Journal* 91 (2017) 291-302  
<http://dx.doi.org/10.1016/j.firesaf.2017.03.036>
  19. Investigation Heat and Smoke Propagation Mechanisms in Multi-Compartment Fire Scenarios, Final Report of the PRISME project, NEA/CSNI/R(2017)14, January 2018
  20. Zavaleta P, Audouin L. Cable tray fire tests in a confined and mechanically ventilated facility. *Fire and Materials*. 2018;42:28–43. <https://doi.org/10.1002/fam.2454>
  21. IEC 60332-1-2, Tests on electric and optical fibre cables under fire conditions - Part 1-2: Test for vertical flame propagation for a single insulated wire or cable - Procedure for 1 kW pre-mixed flame, International Electrotechnical Commission (IEC)
  22. NF C 32-070, Classification tests for conductors and cables in terms of their fire behavior, January 2001, AFNOR
  23. EN 13501-6:2014, Fire classification of construction products and building elements. Part 6: Classification using data from reaction to fire tests on electric cables
  24. Drysdale, D., 2004, An introduction to fire dynamics, 2nd Ed., John Wiley & Sons Ltd, ISBN 0-

471-97290-8

25. EN 61034-2:2005+A1:2013, Measurement of smoke density of cables burning under defined conditions. Test procedure and requirements
26. Coutin, M., Plumecocq, W., Melis, S., Audouin, L., 2012, Energy balance in a confined fire compartment to assess the heat release rate of an electrical cabinet fire, *Fire Safety Journal*, 52, p34-45
27. Pretrel, H., Le Saux, W., Audouin, L., 2013, Experimental determination of fire heat release rate with OC and CDG calorimetry for ventilated compartments fire scenario, *Fire and Materials*, 38, p474-506
28. Brohez, S., Marlair, G., Tewarson, A., 1998, Accurate Calculations of the Heat Release in Fires, 13th International Congress of Chemical and Process Engineering, Prague, paper n°1363
29. Zavaleta P, Suard S, Audouin L. Fire spread from an open-doors electrical cabinet to neighboring targets in a confined and mechanically ventilated facility. *Fire and Materials*. 2018;1–20. <https://doi.org/10.1002/fam.2685>
30. JCGM 100:2008(F) GUM 1995, Evaluation of measurement data – Guide to the expression of uncertainty in measurement, September 2008
31. ISO/DIS 16733-1 - Fire safety engineering – Selection of design fire scenarios and design fires – Part 1: Selection of design fire scenarios, ISO/DIS 16733-1:2014(E)
32. Tewarson, A., 2002, Generation of Heat and Chemical Compound in Fires, SFPE handbook of Fire Protection Engineering, ISBN:087765-451-4, Third edition, Section three, Chapter 4
33. Zavaleta, P., Bascou, S., Suard, S., 2017, Effects of cable tray configuration on fire spread, Proceeding of the fifteenth international Fire and Materials conference, San Francisco, USA, p17-30
34. Croft, W., M., Fires involving Explosions – A literature review, *Fire Safety Journal*, 3 (1980/81) 3 - 24
35. Dobashi, R., Studies on accidental gas and dust explosions, IAFSS 12<sup>th</sup> Symposium 2017, *Fire Safety Journal* 91 (2017) 21-27, <http://dx.doi.org/10.1016/j.firesaf.2017.04.029>
36. Zalosh, R., 2002, Explosion Protection, SFPE handbook of Fire Protection Engineering, ISBN:087765-451-4, Third edition, Section three, Chapter 16

## List of tables

Table 1: Cable tray (CT) tests of the OECD PRISME-2 project considered in this study. ....	16
Table 2: Electric cables A and B used for the CT1/CT2 and the CT3/CT4/CT5 tests, respectively. ....	17
Table 3: Thermophysical properties at ambient temperature (20 °C) of the outer sheath for the cable B. ....	18
Table 4: Consequences of the C <sub>n</sub> H <sub>m</sub> ignitions highlighted for the CT2, CT4 and CT5 tests. ....	19
Table 5: HRR peaks and growth rates of both the cable tray fires and C <sub>n</sub> H <sub>m</sub> ignitions (1) to (6) for the CT2, CT4 and CT5 tests. ....	20
Table 6: Fire characteristics of cable tray fires of the CT1 to CT5 tests. ....	21

## List of figures

Fig. 1: Vertical stack of five horizontal ladder cable trays. ....	22
Fig. 2: Loose arrangement of the electric cables (CT2 test). ....	23
Fig. 3: Electric cables used for the PRISME-2 CT tests. (a). Cable A. (b). Cable B. ....	24
Fig. 4: Perspective view of the DIVA facility. ....	25
Fig. 5: Front view of the experimental facility: Room 1 as the fire room (FR) and Room 2 as the adjacent room (AR). ....	26
Fig. 6: Top view of the experimental facility: Room 1 as the fire room (FR) and Room 2 as the adjacent room (AR). ....	26
Fig. 7: Enlarged view of the SE corner (FR). (a) Vertical profile of nine thermocouples. (b) Gas sampling probes for the measurement of O <sub>2</sub> , CO <sub>2</sub> , CO and C <sub>n</sub> H <sub>m</sub> concentrations. ....	27
Fig. 8: Two scales below the trays and the heat flux sensor (HF) in the upper part of the FR. ....	28
Fig. 9: Cable trays during and after the CT2 test. (a) to (e) during fire. (a) t = 30 s. (b) t = 1 min. (c) t = 2 min. (d) t = 3 min. (e) t = 4 min. (f) after fire. ....	29
Fig. 10: Cable trays for the CT4 test. (a) before fire. (b) after fire. ....	29
Fig. 11: Cable trays for the CT5 test. (a) before fire. (b) after fire. ....	29
Fig. 12: Gas temperatures in the NW corner of the FR. (a) CT2 test. (b) CT4 test. (c) CT5 test. ....	30
Fig. 13: Gas temperatures in the NE corner of the FR. (a) CT2 test. (b) CT4 test. (c) CT5 test. ....	30
Fig. 14: Gas temperatures in the SE corner of the FR. (a) CT2 test. (b) CT4 test. (c) CT5 test. ....	30
Fig. 15: CO <sub>2</sub> concentration in the FR. (a) CT2 test. (b) CT4 test. (c) CT5 test. ....	31
Fig. 16: O <sub>2</sub> concentration in the FR. (a) CT2 test. (b) CT4 test. (c) CT5 test. ....	31
Fig. 17: C <sub>n</sub> H <sub>m</sub> concentration in the upper part of the FR and at the outlet of the AR. (a) CT2 test. (b) CT4 test. (c) CT5 test. ....	31
Fig. 18: Soot mass concentrations in the FR and AR. (a) CT2 test. (b) CT4 test. (c) CT5 test. ....	32
Fig. 19: Soot mass concentrations in the FR and AR measured during additional cable tray fire tests of the OECD PRISME-2 project which used a HFFR cable type [20]. (a) VRR of 4 h <sup>-1</sup> . (b) VRR of 15 h <sup>-1</sup> . ....	32
Fig. 20: Pressure in the FR and AR. (a) CT2 test. (b) CT4 test. (c) CT5 test. ....	33
Fig. 21: Volume flow rates at the inlet of the FR. (a) CT2 test. (b) CT4 test. (c) CT5 test. ....	33
Fig. 22: Mass loss rate. (a) CT2 test. (b) CT4 test. (c) CT5 test. ....	34
Fig. 23: Heat flux in the upper part of the FR. (a) CT2 test. (b) CT4 test. (c) CT5 test. ....	35
Fig. 24: HRR assessments from the thermal and CDG methods. (a) CT2 test. (b) CT4 test. (c) CT5 test. ....	36
Fig. 25: Final heat release rate. (a) CT2 test. (b) CT4 test. (c) CT5 test. ....	37
Fig. 26: Growth rates for CT2 test. (a) Cable tray fire. (b) C <sub>n</sub> H <sub>m</sub> ignition (1). (c) C <sub>n</sub> H <sub>m</sub> ignition (2). ....	38
Fig. 27: Growth rates for CT4 test. (a) Cable tray fire. (b) C <sub>n</sub> H <sub>m</sub> ignition (3). (c) C <sub>n</sub> H <sub>m</sub> ignition (4). ....	38
Fig. 28: Growth rates for CT5 test. (a) Cable tray fire. (b) C <sub>n</sub> H <sub>m</sub> ignition (5). (c) C <sub>n</sub> H <sub>m</sub> ignition (6). ....	38
Fig. 29: CT1 and CT2 tests (cable A). (a) Mass loss rate. (b) Heat release rate. ....	39
Fig. 30: CT3 to CT5 tests (cable B). (a) Mass loss rate. (b) Heat release rate. ....	39



Table 1: Cable tray (CT) tests of the OECD PRISME-2 project considered in this study.

Test ID <sup>6</sup>	Cable ID	Conditions
CT1	Cable A	Open atmosphere
CT2	Cable A	CV (VRR = 4 h <sup>-1</sup> )
CT3	Cable B	Open atmosphere
CT4	Cable B	CV (VRR = 15 h <sup>-1</sup> )
CT5	Cable B	CV (VRR = 4 h <sup>-1</sup> )

Abbreviations: CT, cable trays; CV, confined and mechanically-ventilated; VRR, ventilation renewal rate.

---

<sup>6</sup> Initial names of the CT1 to CT5 tests, as specified as part of the OECD PRISME-2 project, were CFSS-1, CFS-1, CFSS-4, CFS-2 and CORE-7 respectively.

Table 2: Electric cables A and B used for the CT1/CT2 and the CT3/CT4/CT5 tests, respectively.

<b>Cable ID</b>	<b>Cable material</b>	<b>Outer diameter (mm)</b>	<b>Linear mass density (kg/m)</b>	<b>Supplier reference</b>
Cable A	Poly(vinyl chloride), phthalates and mineral loads such as calcium carbonate (CaCO <sub>3</sub> )	13	235	MCMK 3x2.5 mm <sup>2</sup>
Cable B		14.5	330	SHCVV 8x2 mm <sup>2</sup>

Table 3: Thermophysical properties at ambient temperature (20 °C) of the outer sheath for the cable B.

<b>Thermophysical properties</b>	<b>Outer sheath</b>
Specific heat, $c$ (J.kg <sup>-1</sup> .K <sup>-1</sup> )	1280
Density, $\rho$ (kg/m <sup>3</sup> )	1336
Thermal conductivity, $\lambda$ (W.m <sup>-1</sup> .K <sup>-1</sup> )	0.156

Table 4: Consequences of the C<sub>n</sub>H<sub>m</sub> ignitions highlighted for the CT2, CT4 and CT5 tests.

C <sub>n</sub> H <sub>m</sub> ignition	Test ID	Pressure peak (hPa)	Minimal flow rate at the inlet (m <sup>3</sup> /h)	Combustion zone of the C <sub>n</sub> H <sub>m</sub> in the the FR
1	CT2	145	- 4810 <sup>♦</sup> (960 <sup>*</sup> )	Entire upper part <sup>^</sup>
2	CT2	72	- 3010 (960 <sup>*</sup> )	In the SE and NW corners, under the ceiling
3	CT4	8	2720 (3600 <sup>*</sup> )	In the NW corner, under the ceiling
4	CT4	12	2290 (3600 <sup>*</sup> )	In the NW corner, under the ceiling
5	CT5	10	210 (960 <sup>*</sup> )	In the NW corner, under the ceiling
6	CT5	135	- 4710 (960 <sup>*</sup> )	Entire upper part <sup>^</sup>

<sup>♦</sup>Values of measured flow rate at the inlet were negative (i.e., in the reversed direction than the nominal ventilation flow rate) when smoke exited from the FR caused by the overpressure.

<sup>\*</sup>Nominal value of the ventilation flow rate at the inlet.

<sup>^</sup>This zone covers all the ceiling of the FR over a gas layer higher than 1 m depth.

Table 5: HRR peaks and growth rates of both the cable tray fires and  $C_nH_m$  ignitions (1) to (6) for the CT2, CT4 and CT5 tests.

<b>Test ID</b>	<b>Growth rate, <math>\alpha</math> (kW/s<sup>2</sup>)</b>	<b>Growth characteristic time, <math>t_1</math> (s)</b>	<b>HRR peak (MW)</b>
<b>CT2</b>			
<i>Cable tray fire</i>	0.16	79	0.98
<i>C<sub>n</sub>H<sub>m</sub> ignition (1)</i>	5.6	13.4	1.34
<i>C<sub>n</sub>H<sub>m</sub> ignition (2)</i>	5.5	13.5	0.54
<b>CT4</b>			
<i>Cable tray fire</i>	0.022	213	0.75
<i>C<sub>n</sub>H<sub>m</sub> ignition (3)</i>	0.22	67	0.31
<i>C<sub>n</sub>H<sub>m</sub> ignition (4)</i>	0.23	66	0.50
<b>CT5</b>			
<i>Cable tray fire</i>	0.037	164	0.57
<i>C<sub>n</sub>H<sub>m</sub> ignition (5)</i>	0.08	112	0.45
<i>C<sub>n</sub>H<sub>m</sub> ignition (6)</i>	35	5.35	1.75

Table 6: Fire characteristics of cable tray fires of the CT1 to CT5 tests.

Test ID	Cable ID	Conditions	MLR peak (g/s)	HRR peak (MW) <sup>♦</sup>	$\overline{\Delta H_{c,eff}}$ (MJ/kg)	$\xi$ (-)
CT1	Cable A	Open	156	3.20	22.5	-
CT2	Cable A	CV (4 h <sup>-1</sup> )	100	0.98	13	0.58
CT3	Cable B	Open	176	2.70	17	-
CT4	Cable B	CV (15 h <sup>-1</sup> )	58	0.75	12.5	0.74
CT5	Cable B	CV (4 h <sup>-1</sup> )	62 <sup>*</sup>	0.57	8	0.47

Abbreviations: CT, Cable trays; CV, Confined and mechanically-ventilated; MLR, mass loss rate; HRR, heat release rate;  $\overline{\Delta H_{c,eff}}$ , average effective heat of combustion;  $\xi$ , combustion efficiency ratio.

<sup>♦</sup>HRR peak of the cable tray fire.

<sup>\*</sup>The higher MLR peak for CT5 test (VRR = 4 h<sup>-1</sup>) than for CT4 test (VRR = 15 h<sup>-1</sup>) is explained by the feed-back effect on the MLR showed for the first test, as discussed in section 3.3.1.

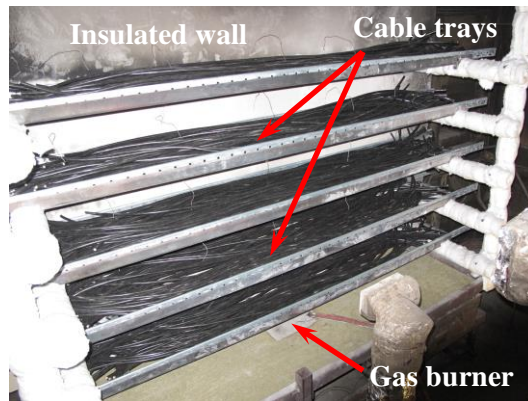
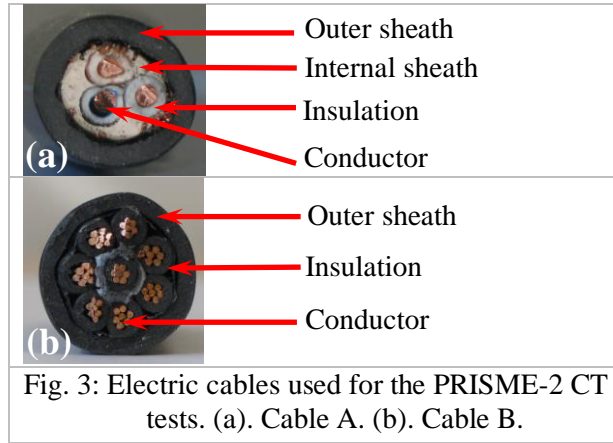


Fig. 1: Vertical stack of five horizontal ladder cable trays.



Fig. 2: Loose arrangement of the electric cables (CT2 test).





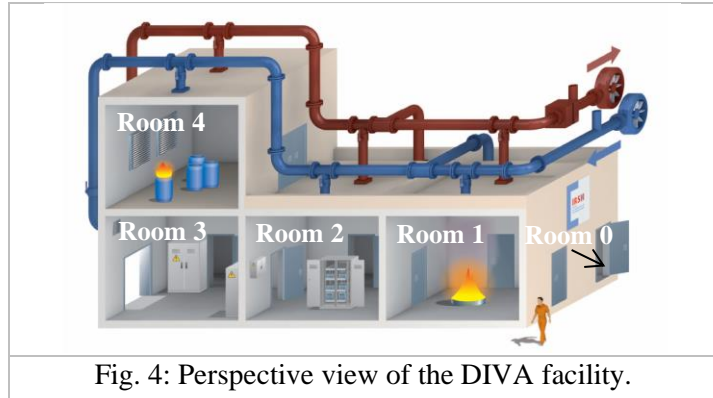


Fig. 4: Perspective view of the DIVA facility.

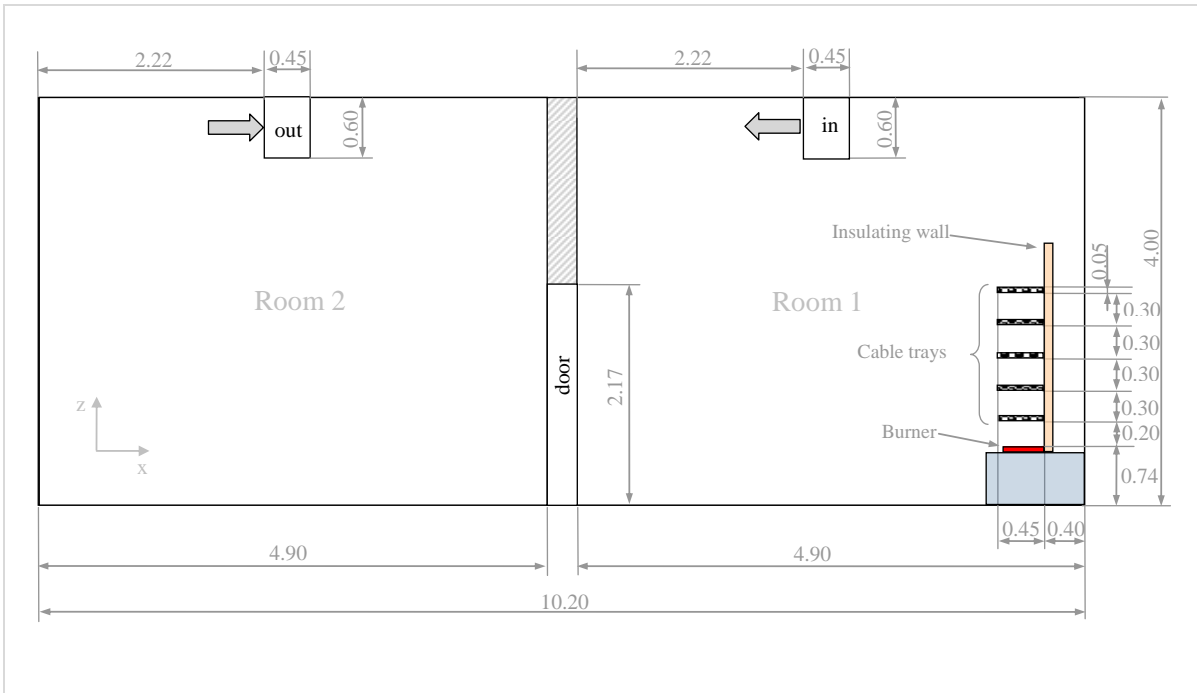


Fig. 5: Front view of the experimental facility: Room 1 as the fire room (FR) and Room 2 as the adjacent room (AR).

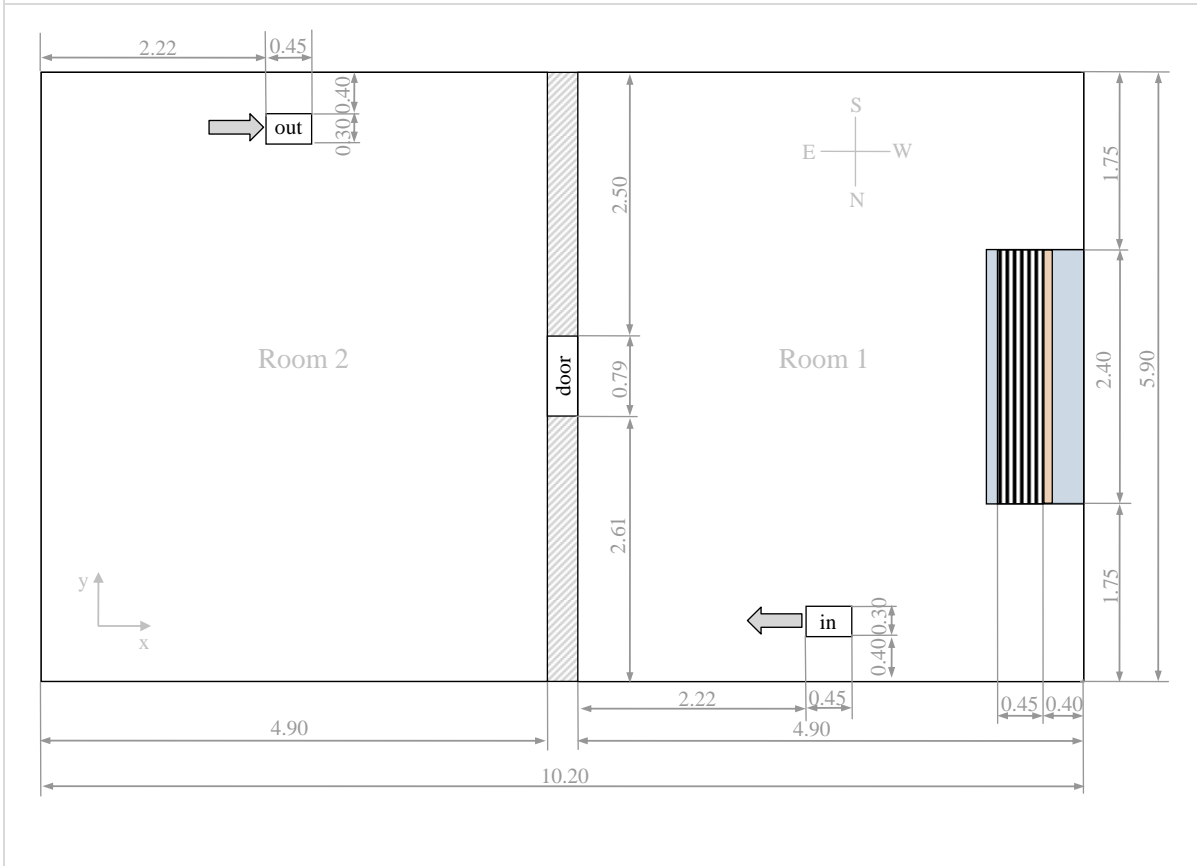


Fig. 6: Top view of the experimental facility: Room 1 as the fire room (FR) and Room 2 as the adjacent room (AR).

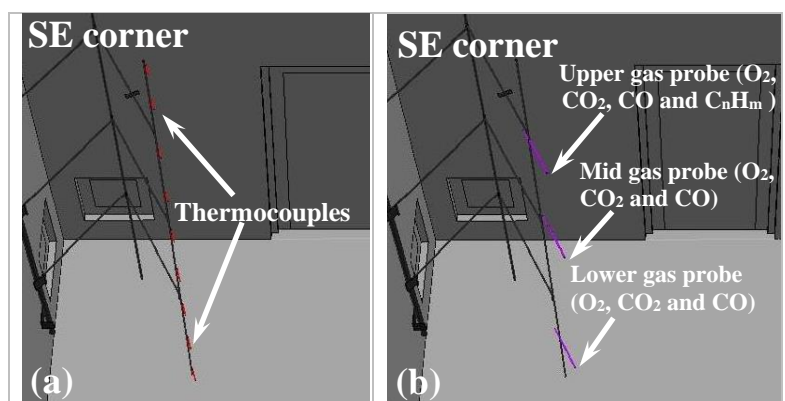


Fig. 7: Enlarged view of the SE corner (FR). (a) Vertical profile of nine thermocouples. (b) Gas sampling probes for the measurement of O<sub>2</sub>, CO<sub>2</sub>, CO and C<sub>n</sub>H<sub>m</sub> concentrations.

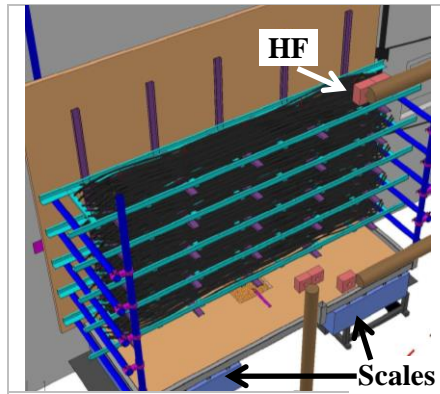


Fig. 8: Two scales below the trays and the heat flux sensor (HF) in the upper part of the FR.



Fig. 9: Cable trays during and after the CT2 test. (a) to (e) during fire. (a)  $t = 30$  s. (b)  $t = 1$  min. (c)  $t = 2$  min. (d)  $t = 3$  min. (e)  $t = 4$  min. (f) after fire.

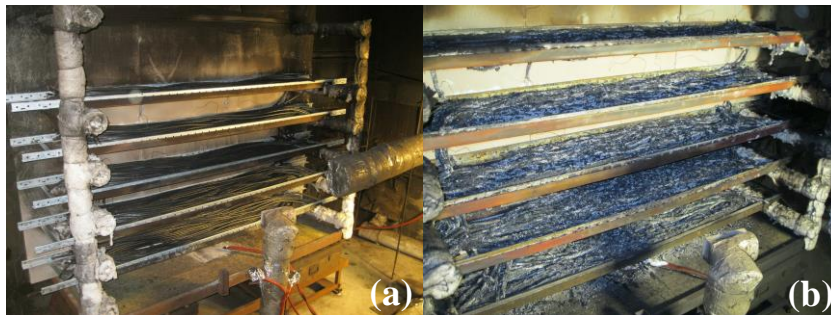


Fig. 10: Cable trays for the CT4 test. (a) before fire. (b) after fire.



Fig. 11: Cable trays for the CT5 test. (a) before fire. (b) after fire.

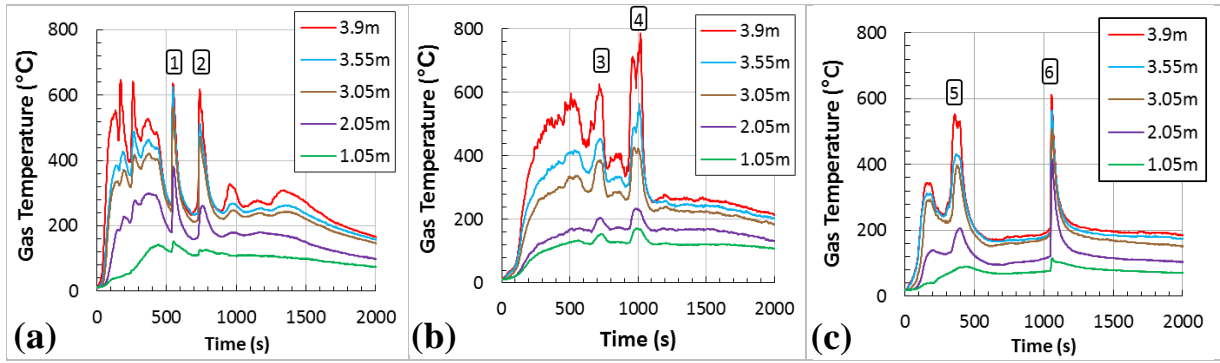


Fig. 12: Gas temperatures in the NW corner of the FR. (a) CT2 test. (b) CT4 test. (c) CT5 test.

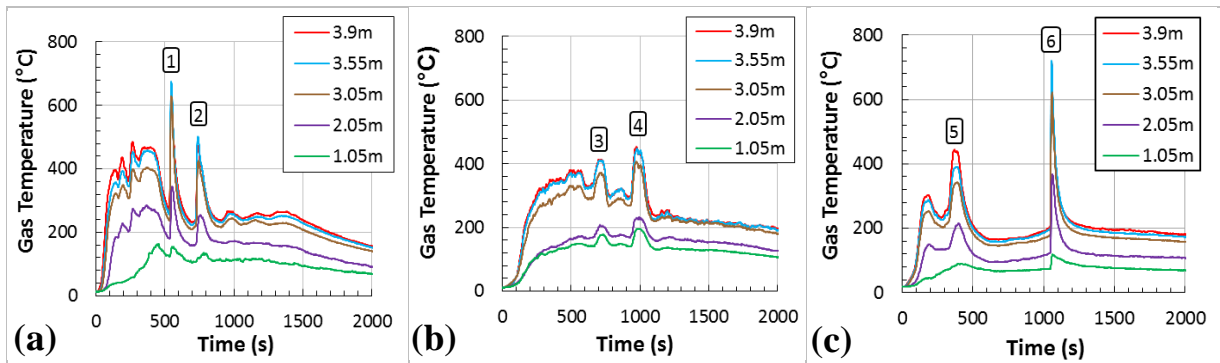


Fig. 13: Gas temperatures in the NE corner of the FR. (a) CT2 test. (b) CT4 test. (c) CT5 test.

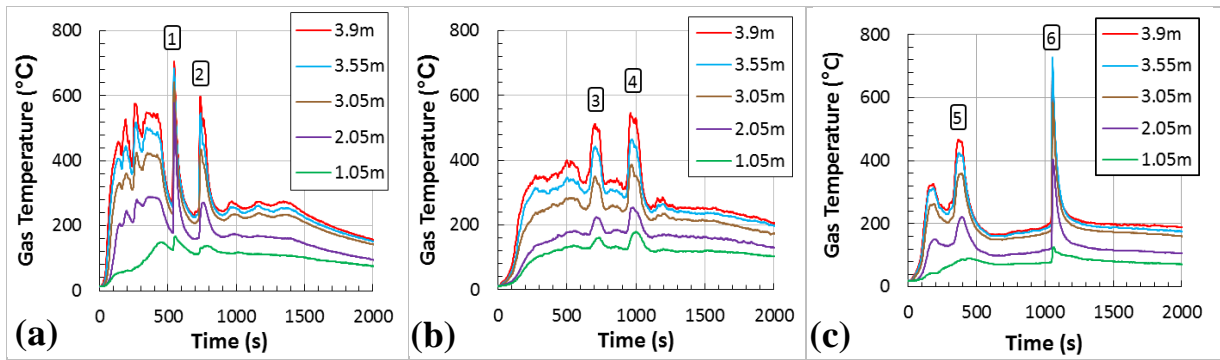


Fig. 14: Gas temperatures in the SE corner of the FR. (a) CT2 test. (b) CT4 test. (c) CT5 test.

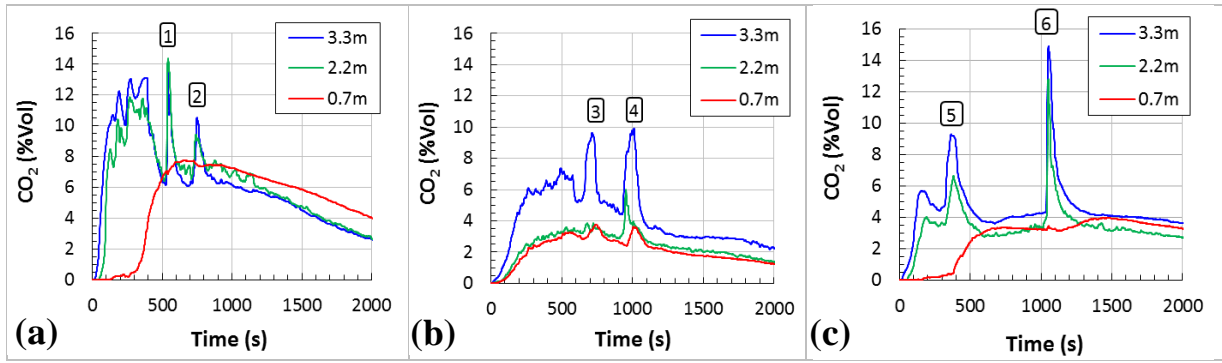


Fig. 15: CO<sub>2</sub> concentration in the FR. (a) CT2 test. (b) CT4 test. (c) CT5 test.

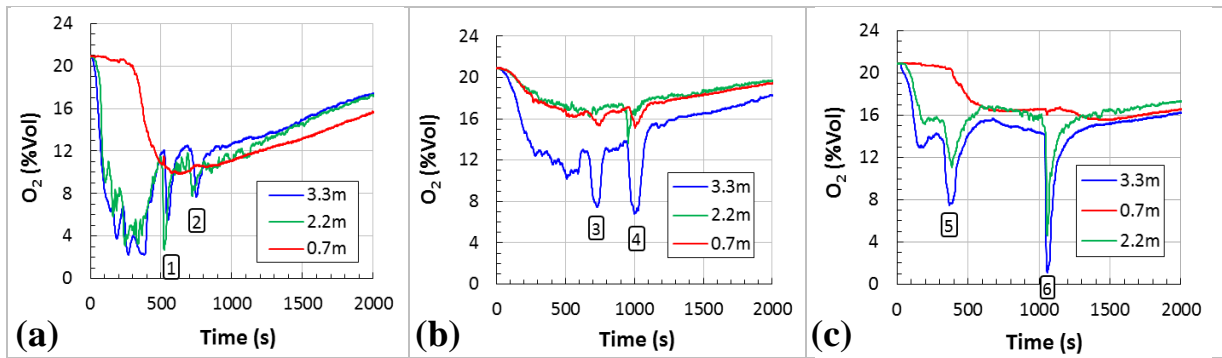


Fig. 16: O<sub>2</sub> concentration in the FR. (a) CT2 test. (b) CT4 test. (c) CT5 test.

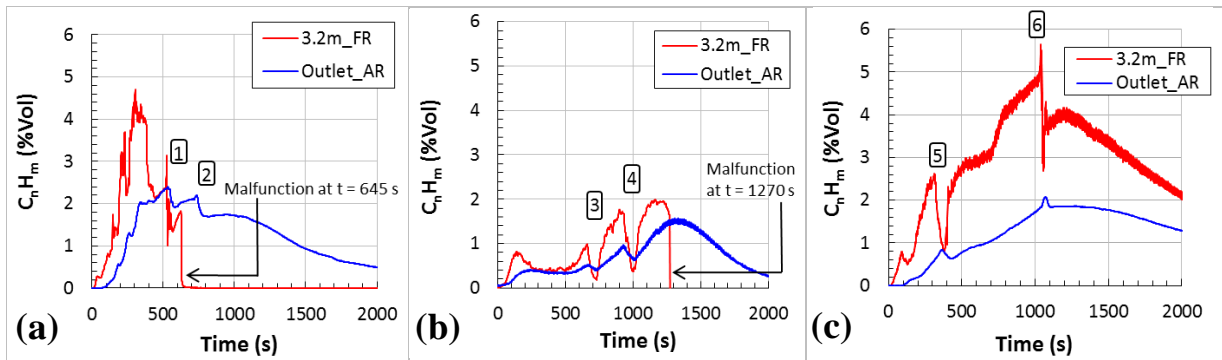


Fig. 17: C<sub>n</sub>H<sub>m</sub> concentration in the upper part of the FR and at the outlet of the AR. (a) CT2 test. (b) CT4 test. (c) CT5 test.



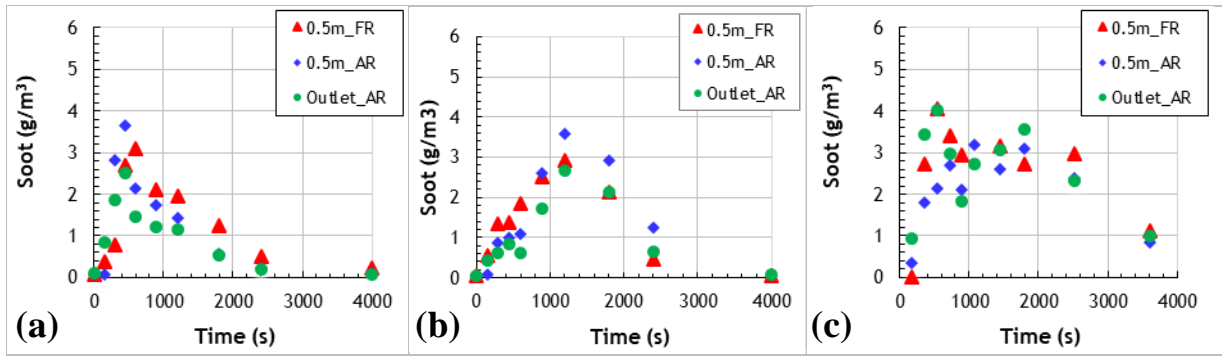


Fig. 18: Soot mass concentrations in the FR and AR. (a) CT2 test. (b) CT4 test. (c) CT5 test.

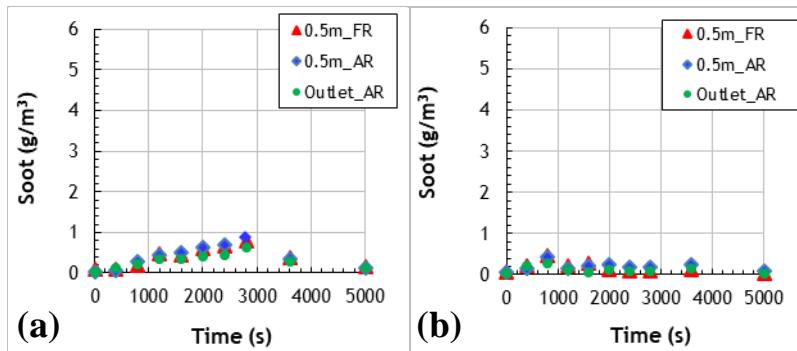


Fig. 19: Soot mass concentrations in the FR and AR measured during additional cable tray fire tests of the OECD PRISME-2 project which used a HFFR cable type. (a) VRR of  $4 \text{ h}^{-1}$ . (b) VRR of  $15 \text{ h}^{-1}$ .

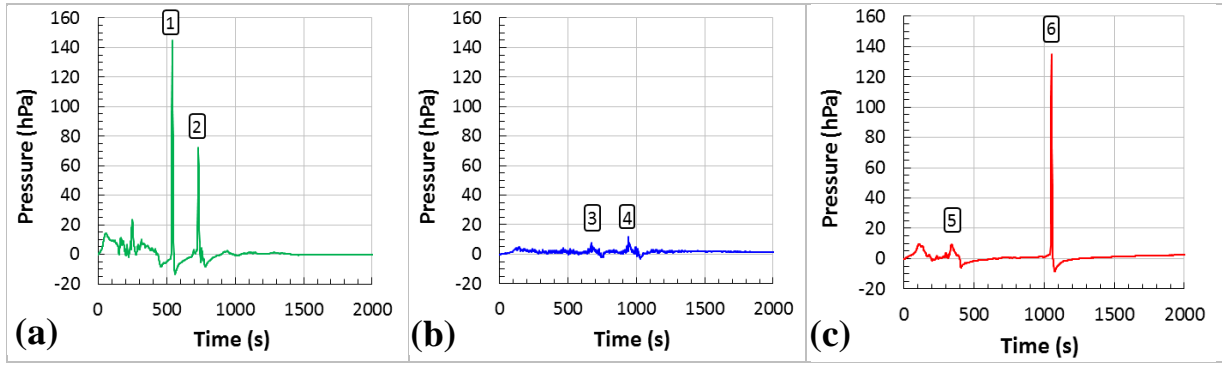


Fig. 20: Pressure in the FR and AR. (a) CT2 test. (b) CT4 test. (c) CT5 test.

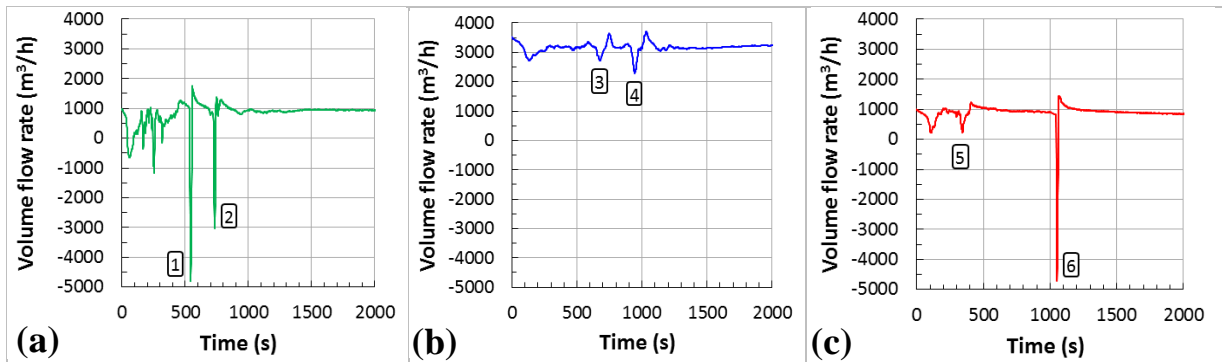


Fig. 21: Volume flow rates at the inlet of the FR. (a) CT2 test. (b) CT4 test. (c) CT5 test.

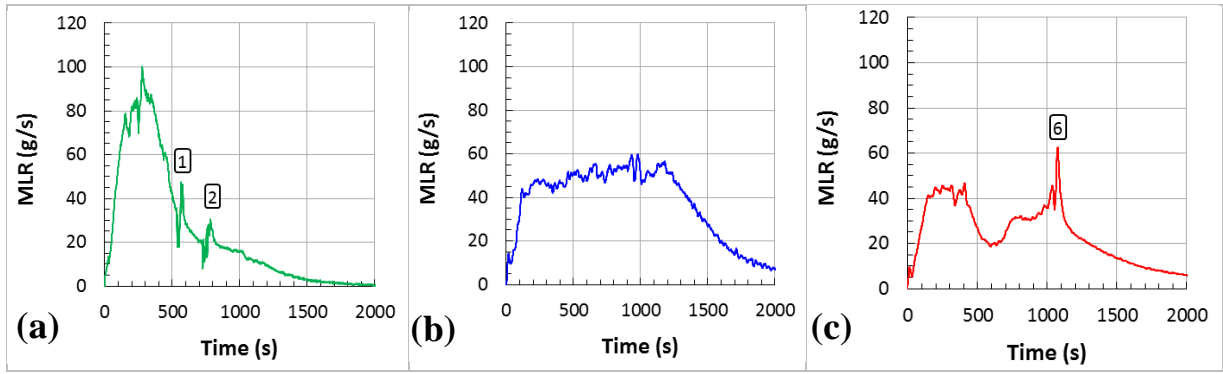


Fig. 22: Mass loss rate. (a) CT2 test. (b) CT4 test. (c) CT5 test.

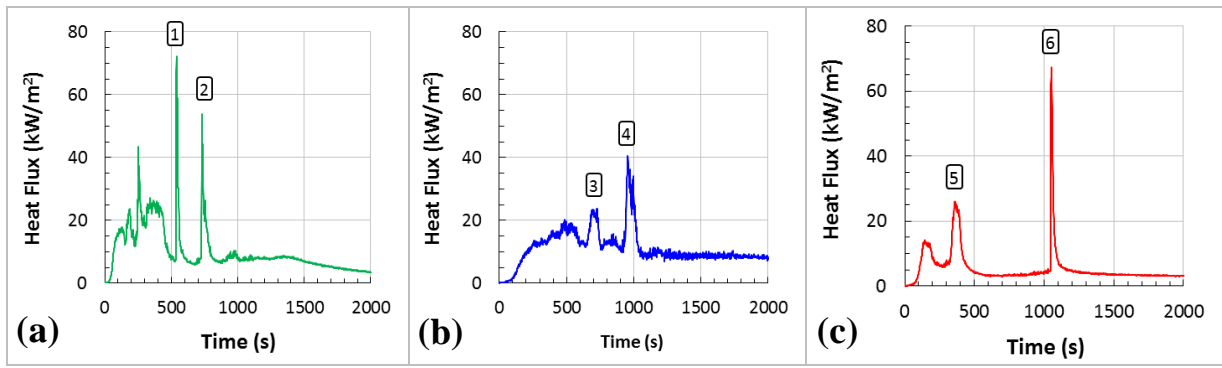


Fig. 23: Heat flux in the upper part of the FR. (a) CT2 test. (b) CT4 test. (c) CT5 test.

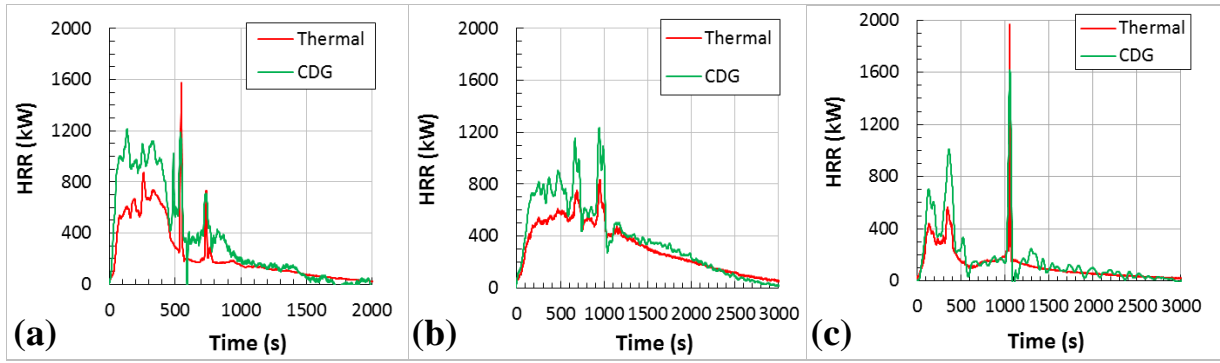


Fig. 24: HRR assessments from the thermal and CDG methods. (a) CT2 test. (b) CT4 test. (c) CT5 test.

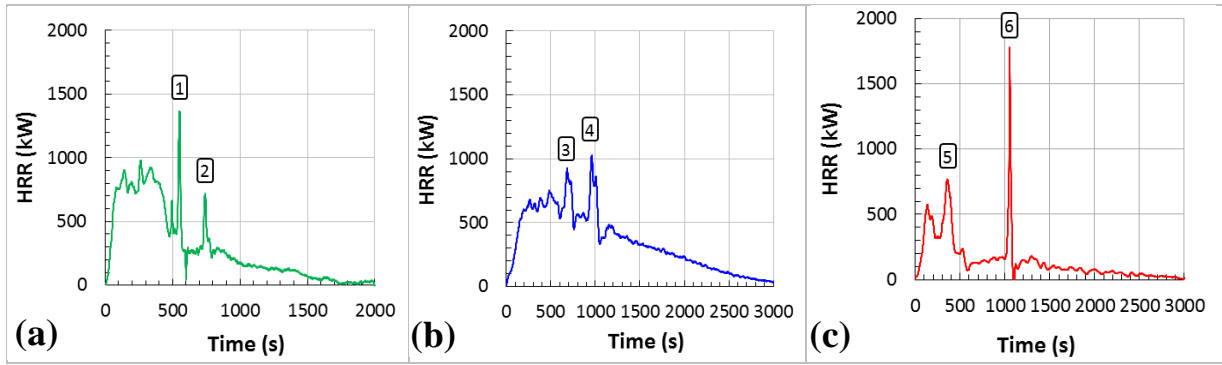


Fig. 25: Final heat release rate. (a) CT2 test. (b) CT4 test. (c) CT5 test.

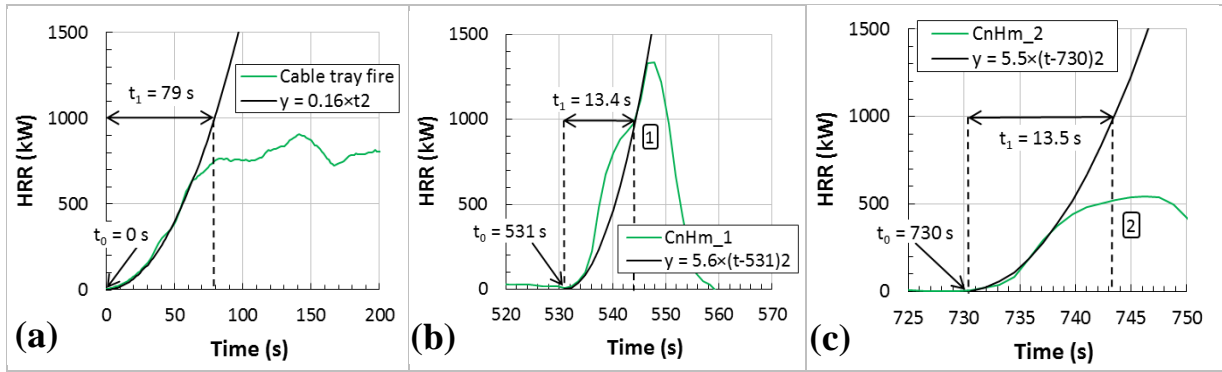


Fig. 26: Growth rates for CT2 test. (a) Cable tray fire. (b) C<sub>n</sub>H<sub>m</sub> ignition (1). (c) C<sub>n</sub>H<sub>m</sub> ignition (2).

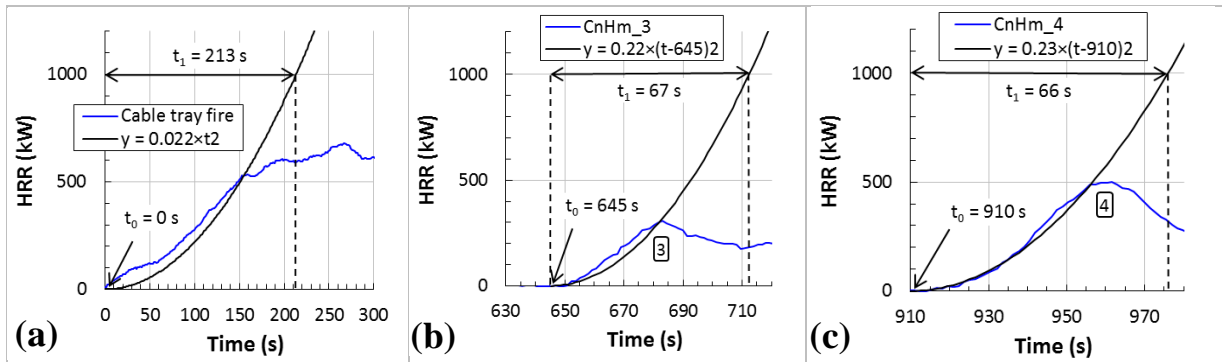


Fig. 27: Growth rates for CT4 test. (a) Cable tray fire. (b) C<sub>n</sub>H<sub>m</sub> ignition (3). (c) C<sub>n</sub>H<sub>m</sub> ignition (4).

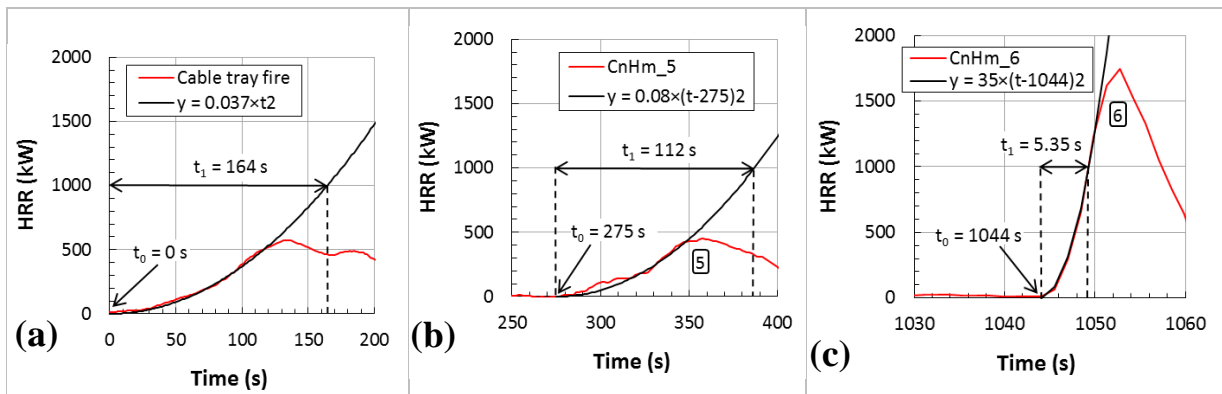


Fig. 28: Growth rates for CT5 test. (a) Cable tray fire. (b) C<sub>n</sub>H<sub>m</sub> ignition (5). (c) C<sub>n</sub>H<sub>m</sub> ignition (6).

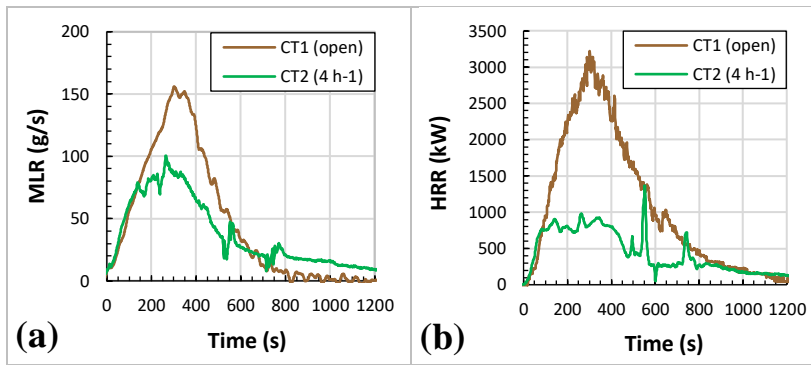


Fig. 29: CT1 and CT2 tests (cable A). (a) Mass loss rate. (b) Heat release rate.

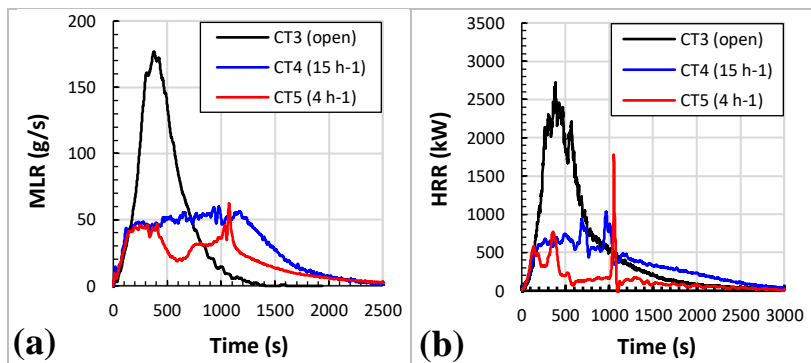


Fig. 30: CT3 to CT5 tests (cable B). (a) Mass loss rate. (b) Heat release rate.